EVALUATION OF BOND STRENGTH OF GRADE 100 REINFORCING BARS

BY

Shelby Miller

Submitted to the graduate program in Civil Engineering
and to the Graduate Faculty of the University of Kansas
in partial fulfillment of the requirements for the degree
of Master of Science.

David Darwin, Chairman

Committee members

JoAnn Browning

Stan Rolfe

Date Defended: _____

The Thesis Committee for Shelby Miller certifies
That this is the approved Version of the following thesis:

BOND STRENGTH OF GRADE 100 REINFORCING STEEL

Committee:

_____
David Darwin, Chairman

_____

_____

Date approved: _____

ABSTRACT

The bond strength of Grade 100 ASTM A 1035 reinforcing steel manufactured by MMFX Technologies Corp. is evaluated with respect to bond strength equations found in ACI 318-05 and ACI 408R-03. Test specimens are full-scale beam-splice specimens tested in four-point bending to create a constant moment region over the length of the splices. Specimens differed with regard to the level of confinement provided by transverse reinforcement, concrete cover and bar spacing, concrete compressive strength, and bar size. Sixty-nine specimens were tested at three universities – North Carolina State University, the University of Texas at Austin, and the University of Kansas – of which 64 failed in bond and are included in this report.

The results indicate that the development length equation found in ACI 318-05 is not suitable for the design of unconfined or confined splices without the use of a modification factor. The development length equation found in ACI 408R-03 is suitable for analysis purposes for both unconfined and confined splices.

ACKNOWLEDGEMENTS

Thank you to everyone who has made this research possible. Thank you to Dr. David Darwin and Dr. JoAnn Browning for their guidance, patience, and support. It's been a pleasure working with you for the past two and a half years.

Thank you to my parents and the rest of my family for the support they've always given me. Your encouragement and faith in me has kept me going.

Thank you to my fellow students at KU, who were always willing to lend a hand. Thanks in particular to Mike Briggs, who worked with me on this project. I don't know how I would have done it without you.

Thank you to the researchers at the University of Texas and North Carolina State University, whose hard work provided additional data for results and analyses.

Thank you to MMFX Technologies Corporation for providing funding and material support for this project. Additional thanks to Dayton Superior Corporation, W. R. Grace & Co., LRM Industries, Builder's Steel, the Kansas Department of Transportation, and the University of Kansas Department of Civil, Environmental & Architectural Engineering for their support.

TABLE OF CONTENTS

LIST OF TABLES

LIST OF FIGURES

CHAPTER 1

INTRODUCTION

1.1 General

Although strong in compression, concrete possesses very little tensile strength. To be of use in construction, steel reinforcing bars, which are strong in both tension and compression, are used in concrete to carry the tension forces, creating reinforced concrete.

Bond is an important factor in reinforced concrete, as the bond between the concrete and the reinforcing steel transfers the tensile forces from the concrete to the reinforcing steel. Bond force is transferred primarily by friction, chemical adhesion, and mechanical interlock between bar deformations and the surrounding concrete. For deformed bars, which are the most commonly used reinforcing bars, mechanical interlock is the primary method of bond force transfer. Inadequate bond force transfer can cause failure of the concrete by splitting of the concrete near the reinforcing steel or by the reinforcing steel pulling out of the concrete.

To transfer bond force adequately, there must be a sufficient length of reinforcing bar, known as the development length over which the bond force is transferred from the concrete to the reinforcing steel or the splice length over which the bond force is transferred between two spliced bars. The development/splice length required to adequately transfer bond force depends on many factors, including deformation properties of the bar, such as height and spacing, concrete cover, concrete strength, bar size, and confinement by transverse reinforcement.

This study covers the bond behavior of Grade 100 A 1035 reinforcing steel, manufactured by MMFX Technologies Corporation, evaluated at stresses between 80 and 140 ksi. The reinforcing steel is evaluated using beam-splice specimens with 2 to 4 lap splices in each specimen. The specimens were designed to investigate the effects of such factors as confinement level, concrete cover, concrete compressive strength, bar size, and splice strength. Previous research indicates that bond

equations developed for lower strength steels may be unconservative at stresses above 100 ksi (El-Hacha and Rizkalla 2004).

This study is part of joint bond research program between the University of Kansas, the University of Texas at Austin, and North Carolina State University. The program includes tests of sixty-nine beam-splice specimens of which 64 experienced bond failure and are included in this report.

1.2 Previous work

Previous studies show that compared with Grade 60 steel, Grade 100 steel allows beam-splice specimens to reach higher loads and deflections before failure (Ansley 2002). The earlier tests also indicate that for bars not confined by transverse reinforcement, longer splices will increase the load at failure and may provide additional ductility, although after a certain point increasing the splice length will not increase the load or deformation capacity (Peterfreund 2003).

1.2.1 Comparison with Grade 60 Steel

The Florida Department of Transportation (FDOT) conducted a series of tests on four sets of two beams each for the purpose of comparing MMFX Grade 100 reinforcing steel with Grade 60 reinforcing steel (Ansley 2002). All four sets of tests were full scale beam specimens and used concrete with a target compressive strength of 5000 psi. Of the four sets, one used continuous flexural reinforcement, two used unconfined lap splices, and one studied the effects of using Grade 60 stirrups versus Grade 100 stirrups. Only the splice tests are described here.

The first set of lap splice tests used No. 6 reinforcing bars with a lap splice of 10.5 in. at the midspan of the beam. Both the specimen with the Grade 60 reinforcement and the specimen with the Grade 100 reinforcement failed in bond before the bars yielded. Although neither steel yielded, the beam with Grade 100 reinforcement attained a higher load than the beam with Grade 60 reinforcement, reaching a higher load before failure.

The second set of lap splice tests used No. 6 reinforcing bars with a lap splice of 30.5 in. at the midspan of the beam. Both specimens failed in bond, though the stress was high enough to yield the Grade 60 steel before failure. The beam with Grade 100 attained a higher load, and since the steel did not yield, deflected significantly less than beam with Grade 60 steel.

1.2.2 Development length characteristics

Peterfreund (2003) conducted six tests of full scale beam-splice specimens. The specimens contained non-contact lap splices of Grade 100 No. 4 and No. 5 bars with a clear spacing of one bar diameter. Concrete cover of at least 1.5 in. was provided on all sides. Specimens were tested in four-point loading. The concrete compressive strength was approximately 6000 psi.

The three tests conducted with No. 4 bars used splice lengths of 23.8 in., 18.5 in., and 13.8 in. The tests with the two longer splices failed at approximately the same load, but the specimen with the longest splice exhibited more ductility, indicating better bond with the concrete. The specimen with the shortest splice failed at a significantly lower load and exhibited much less ductility.

Of the three tests conducted with No. 5 bars, one was not loaded to failure due to technical problems, and only the remaining two were included in the final data. The two specimens had splice lengths of 37.0 in. and 29.1 in. The specimen with the longer splice failed at a higher load and exhibited greater ductility than that with the shorter splice. Both No. 5 bar test specimens failed at higher loads than the No. 4 bar test specimens, although the specimens containing No. 5 bars did not exhibit significantly greater ductility.

1.2.3 Design Equations

The equations found in ACI 408R-03 (ACI Committee 408 2003) [Eq. (1.1)] and ACI 318-05 (ACI Committee 318 2005) [Eq. (1.2)] can be used to predict bond strength and determine the development length necessary to adequately anchor reinforcing bars. The equations in ACI 408R-03 are more commonly used for

analysis, and take into account bar size, concrete compressive strength, splice length, bottom and side cover, bar spacing, the effects of confining transverse reinforcement, and relative rib area of the bars. The term $\left(\frac{c\omega + K_{tr}}{d_b}\right)$ is limited to 4, as this has been found to be the point at which bond failure begins to transition from splitting to pullout (Darwin 1996b).

Equation (1.1) was developed using a database of more than 450 beam-splice tests dating from 1955. During its development, the original equation factored in the effects of development length, concrete compressive strength, cover, bar diameter, and the amount and spacing of confining transverse reinforcement on bar stress. Research by Darwin, et. al. (1996a), first using a database of 199 beams found that using the quarter power of f_c' more closely approximated the effects of concrete compressive strength than the more commonly used square root of f_c' (Orangun et. al. and ACI 318-05). The new equation also took into account relative rib area of the bar. An improved equation was developed by Zuo and Darwin (2000). It used a larger database, 367 beams, and included the effects of high-strength concrete. It served as the prototype for Eq. (1.1) developed by ACI Committee 408 (2003).

$$\frac{\ell_s}{d_b} = \frac{\left(\frac{f_s}{f_c'^{1/4}} - 2400\omega\right)}{76.3\left(\frac{c\omega + K_{tr}}{d_b}\right)} \tag{1.1}$$

$$\omega = 0.1\frac{c_{\max}}{c_{\min}} + 0.9 \le 1.25 \tag{1.1a}$$

$$c = c_{\min} + 0.5d_b \tag{1.1b}$$

$$K_{tr} = \left(\frac{0.52 t_r t_d A_{tr}}{sn} \right) f_c'^{1/2} \quad (1.1c)$$

$$t_d = 0.72 d_b + 0.28 \quad (1.1d)$$

$$t_r = 9.6 R_r + 0.28 \leq 1.72 \quad (1.1e)$$

where:

A_{tr} = total cross-sectional area of all transverse reinforcement, in^2

c_b = cover of reinforcement being developed, measured to tension face of member, in.

c_{max} = maximum value of c_s or c_b, in.

c_{min} = minimum value of c_s or c_b, in.

c_s = minimum value of c_{si} + 0.25 in. or c_{so}, in.

c_{so} = side cover of reinforcing bars, in.

c_{si} = half the clear spacing between reinforcing bars, in.

d_b = nominal bar diameter, in.

f_c' = specified compressive strength of concrete, psi

f_s = bar stress, psi

ℓ_d = development length, in.; taken as equal to splice length ℓ_s

n = number of bars being developed or spliced along plane of splitting

N = number of stirrups or ties crossing a splice

R_r = relative rib area, ratio of projected rib area normal to bar axis to product of nominal bar perimeter and average center-to-center rib spacing

s = center-to-center spacing of transverse reinforcement within ℓ_d or ℓ_s, taken as ℓ_s/N when when matching tests

Equation (1.2), from ACI 318-05, is used for design. The equation takes into account bar size, concrete compressive strength, splice length, bottom cover, and the effect of confining transverse reinforcement. It was developed based on the work of Orangun et. al. (1995) and first appeared in ACI 318-95 (ACI Committee 318 1995). Because it was meant for design, it gives a more conservative estimate of bar stress than the equation found in ACI 408R-03. The term $\left(\frac{c_b + K_{tr}}{d_b}\right)$ is limited to 2.5.

$$\frac{\ell_d}{d_b} = \frac{3}{40}\frac{f_s}{\sqrt{f'_c}}\frac{\psi_s}{\left(\frac{c_b + K_{tr}}{d_b}\right)} \tag{1.2}$$

$$K_{tr} = \frac{A_{tr} f_{yt}}{1500sn} \tag{1.2a}$$

where:

A_{tr} = total cross-sectional area of all transverse reinforcement, in^2

c_b = cover of reinforcement being developed, measured to tension face of member, in.

d_b = nominal bar diameter, in.

f'_c = specified compressive strength of concrete, psi

f_s = bar stress, psi

f_{yt} = yield strength of the transverse reinforcement, psi

ℓ_d = development length, in.; taken as equal to splice length ℓ_s

n = number of bars being developed or spliced along plane of splitting

s = maximum center-to-center spacing of transverse reinforcement with in ℓ_d or ℓ_s

ψ_s = reinforcement size factor = 1.0 for bar sizes greater than No. 7 and 0.8 for No. 6 and smaller

1.3 Discussion

Bond force is the force transferred between concrete and reinforcing bars in reinforced concrete members (Fig. 1.1). Bond can be affected by many factors including concrete strength, reinforcing bar size and placement, amount of confining transverse reinforcement, and splice or development length.

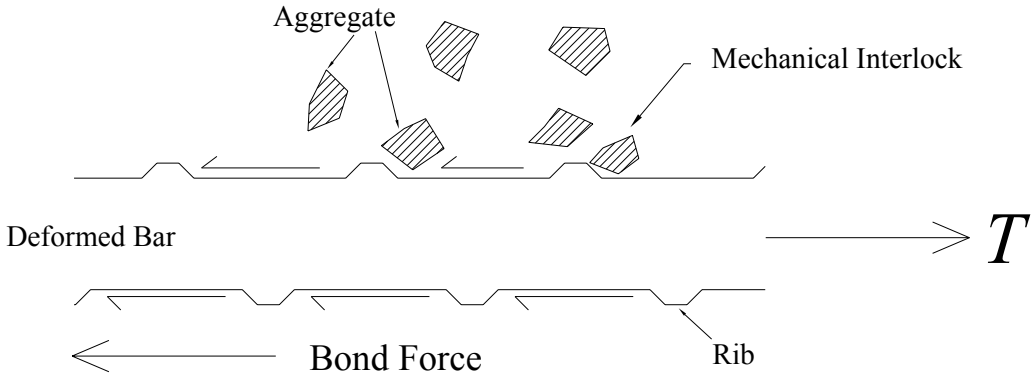

Figure 1.1 - Mechanical interlock between concrete and a reinforcing bar

1.3.1 Bond force

The bond between concrete and reinforcing steel allows tensile stresses in the concrete to be transferred to the reinforcing steel. Adequate bond between concrete and reinforcing steel enables a reinforced concrete member to reach its full flexural design capacity.

Bond force is transferred in three ways - by adhesion, friction, and mechanical interlock. Adhesion is the weakest force, and involves the chemical bond between the concrete and the steel. Adhesion force is lost once the steel slips with respect to the concrete. Friction contributes to the resisting force during slip. Both adhesion and friction decrease when the reinforcing bar is placed in tension because the diameter of the bar tends to decrease slightly due to Poisson's effect. Mechanical interlock between the deformations on the bar and the surrounding concrete provides the majority of the bond force transfer.

1.3.2 Bond failure

Bond failure can occur through splitting or pullout. A splitting failure occurs when the relative movement between the reinforcing steel and the concrete becomes high enough that the deformations on the bar begin to act as wedges, putting the surrounding concrete in transverse tension and causing the formation of splitting cracks parallel to the bar. Splitting cracks typically radiate outward from the bar and tend to first form where there is the least amount of concrete cover. With continued loading, splitting cracks grow in width and radiate outward to the face of the specimen or between adjacent bars or splices. As they continue along the development length of the bar, the cracks can cause the delamination of a layer of concrete unless confining transverse reinforcement is provided. Crack growth eventually leads to bond failure.

A pullout failure occurs when the concrete between the deformations on the bar fails in shear or compression. A pullout failure tends to occur only when the concrete cover is high or the bar is confined by transverse reinforcement that limits the propagation of splitting cracks.

1.3.3 Factors affecting bond

Many factors are known to influence bond strength. Among the more influential are concrete cover, bar spacing, amount of confining transverse reinforcement, splice and development length, concrete compressive strength, bar size, and relative rib area. The effects of splice length and amount of confining transverse reinforcement are the two principal factors studied in this project.

Concrete cover and bar spacing

Concrete cover is the distance between the surface of the bars being developed and the face of the specimen. Cover is typically defined in terms of side cover (cover to the side of the beam) and bottom cover (cover to the tension face of the beam). When determining the required development or splice length, the lowest cover is assumed to control, since that is where the concrete will experience splitting failure

first. Increasing concrete cover can increase the bond force at failure by increasing the confining force on the bar prior to failure. If the cover is high enough, bond failure due to splitting may not occur, and the member may fail in flexure or in bond due to pullout instead.

Because splitting cracks can propagate between bars as well as to the surface of the concrete, closely spaced bars can exhibit reduced bond strength. To help prevent this, bars are typically spaced one or two bar diameters apart in beams. In slabs, which allow greater bar spacing because of their greater widths, shorter development and splice lengths are appropriate. This point is not specifically recognized by Eq. (1.2) but is handled by reducing the development and splice length of bars typically used in slabs, No. 6 and smaller.

Confining transverse reinforcement

Confining transverse reinforcement helps limit the growth of splitting cracks and provides additional clamping force. Confinement reduces the required development and splice length, increases the bond strength, and increases the ductility of the splice. The effectiveness of confining transverse reinforcement depends upon the total cross-sectional area of the transverse steel per deformed bar being developed or spliced.

Development/splice length

Development length is the distance required to fully transfer all of the tensile force in the concrete to the reinforcing steel. If the development length is inadequate, the member may fail in bond before the steel yields. Where lap splices are necessary, the required lap length is the development length needed to fully transfer the tensile force from a bar to the adjoining bar.

Concrete compressive strength

Increasing the compressive strength of concrete increases the tensile strength as well, which helps resist the formation of splitting cracks and increases bond strength. Since the fracture energy of the concrete is not directly related to its compressive strength, an increase in concrete compressive strength does not directly correlate with an increase in bond strength. Rather, bond strength has been found to be more closely related to $\sqrt{f_c'}$ for concretes with compressive strengths less than 8,000 psi and to $\sqrt[4]{f_c'}$ for concretes with compressive strengths from 3,000 to 16,000 psi (ACI Committee 408 2003).

Bar size

Larger reinforcing bars are capable of reaching higher bond forces per unit length than smaller bars for the same cover to the center of the bar or the same confining transverse reinforcement. The increase in bond force in larger bars, however, is not proportional to the increase in bar area. Thus, using a greater number of smaller bars may be more effective than using fewer large bars if the available development length is limited. This will be true until the point at which the closer bar spacing becomes detrimental (ACI Committee 408 2003).

Relative rib area

Relative rib area is the ratio of the bearing area of the bar deformations to the shearing area between the deformations. Relative rib area does not affect the bond strength of bars that are not confined by transverse reinforcement since all modern deformed bars are able to mobilize the splitting strength of the concrete regardless of the size or spacing of the deformations (ACI Committee 408 2003). For bars with confining transverse reinforcement, increasing the relative rib area increases the effectiveness of the confining transverse reinforcement by mobilizing a higher clamping force (Darwin and Graham 1993).

1.3.4 MMFX Grade 100 reinforcing steel

Micro-composite Multi-structural Formable (MMFX) Grade 100 reinforcing steel possesses both increased corrosion resistance (as compared to standard A 615 steel) and high tensile strength. Grade 100 steel has a nominal yield strength of 100 ksi and a nominal tensile strength of 150 ksi. The steel also has a relatively high chromium content, 8-10%, just below that of stainless steel (El-Hacha and Rizkalla 2002) and a low carbon content, required by ASTM A 1035 (2006) to be less than 0.15%. Unlike most ASTM A 615 steel, Grade 100 A 1035 steel lacks a distinct yield point or yield plateau, but instead has a roundhouse curve, as can be seen in Figure 1.2.

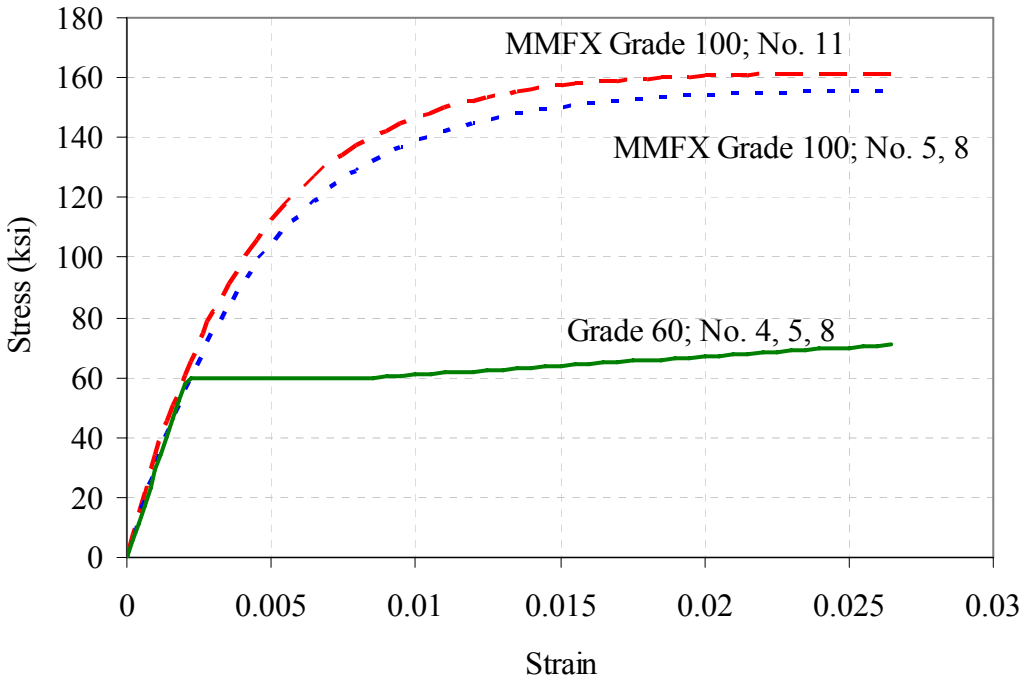

Figure 1.2 - Stress-strain curves of Grade 60 and Grade 100 steels

1.4 Objective and scope

Traditional design and analysis equations such as those found in ACI 318-05 and ACI 408R-03 were calibrated with data from conventional steels with nominal yield strengths of 75 ksi or less. The objective of this research is to evaluate the bond performance of Grade 100 ASTM A 1035 reinforcing steel and determine suitability of the previously established bond design and analysis equations for Grade 100 steel, which can achieve bar stresses of 150 ksi or more.

Three universities, the University of Kansas (KU), the University of Texas at Austin (UT), and North Carolina State University (NCSU), constructed a total of 69 full scale beam-splice specimens designed to fail at tension bar stresses of 80, 100, 120, or 140 ksi. The specimens were designed in flexure to reach tensile bar stresses of 150 ksi before failing in flexure. The specimens were designed with varying concrete cover, concrete compressive strength, splice length, bar size, and amount of confining transverse reinforcement to determine the effect of these parameters on the bond strength of the steel.

Of the 69 specimens, ten were cast as slab specimens with four lap splices each, while 59 were beams with two lap splices. Twelve beams had duplicate specimens cast at other universities for purposes of comparison. KU and NSCU each tested 22 beam-splice specimens, while UT cast an additional three specimens to study the effect of concrete compressive strength on bond strength for a total of 25 specimens. Of 69 beams cast at three universities, 64 failed in bond and are included in this report. Detailed test results for the KU specimens can be found in Appendix B.

CHAPTER 2

EXPERIMENTAL PROGRAM

2.1 General

As recommended by ACI Committee 408 (2003), beam-splice specimens were used to study the bond behavior of the reinforcing steel. The specimens tested at the University of Kansas were designed to achieve a stress in the tension steel of 150 ksi at flexural failure. Splice lengths, confining transverse reinforcement, and concrete cover dimensions were selected to achieve a bond failure within the splice at stress levels in the tension steel of 80, 100, 120, or 140 ksi based on bond strength prediction equations in ACI 408R-03 (ACI Committee 408 2003).

Of the sixty-nine beams tested in the study, twenty-two specimens were tested at the University of Kansas (KU) with the following parameters:

No. 5 bars:

- ¾ in. and $2d_b$ cover
- 18, 25, 32, and 43 in. splice lengths, ℓ_s
- 5000 psi target concrete compressive strength, f_c'
- All splices unconfined

No. 8 bars:

- 1 ½ in. and 2 ½ in. cover
- 27, 36, 47, and 63 in. splice lengths, ℓ_s
- 5000 and 8000 psi target concrete compressive strength, f_c'
- 0, 2, 4, 5, and 8 No. 4 bar stirrups confining the splice

No. 11 bars:

- 2 in. cover
- 58 and 79 in. splice lengths, ℓ_s
- 8000 psi target concrete compressive strength, f_c'
- 0, 4, and 9 No. 4 bar stirrups confining the splice

2.1.1 Notation

Test specimens are identified using a notation system common to the three universities. The notation designates the size of the spliced bars, the concrete compressive strength in ksi, the bar stress level for splices without confining steel, the level of confinement, and the concrete clear cover. Beams were designed in groupings of six with identical cover, dimensions, and span lengths. The beams in a series differ in terms of splice length (two lengths were used) and level of confinement (three levels were used). Beams are identified as shown in Figure 2.1 and described in Section 2.1.2.

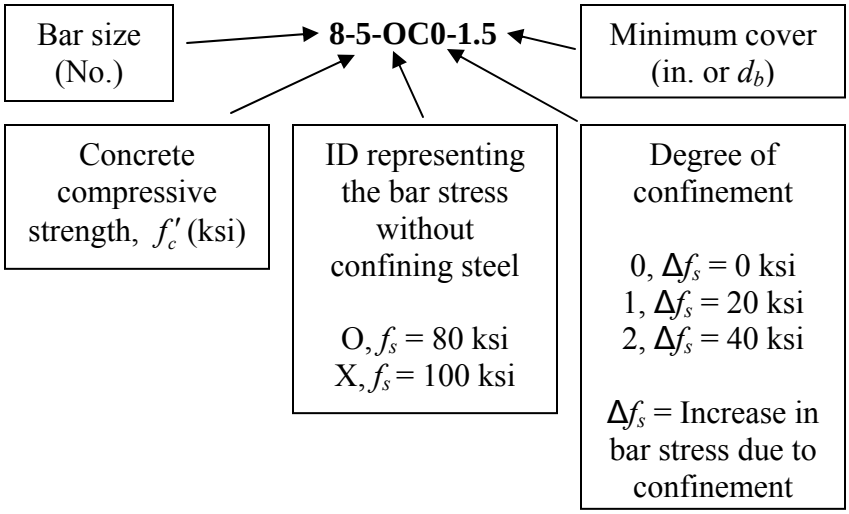

Figure 2.1 - Sample notation for a beam-splice specimen

2.1.2 Collective Test Program

Each school was responsible for three series of specimens plus two sets of two beams from a series for which another university had primary responsibility. Table 2.1 summarizes the test program. Duplicate beams are shown in bold. The test specimens include those from the original program of sixty-six beams plus three extra specimens tested at the University of Texas (UT) for the purpose of evaluating the

effect of concrete compressive strength. These specimens are duplicates of specimen 8-8-OC_-1.5 at the 0, 1, and 2 levels of confinement, but were cast with 5 ksi concrete instead of 8 ksi concrete. To avoid confusion with specimens already titled 8-5-OC_-1.5, which have a different splice length, these three additional specimens are designated as 8-5-SC_-1.5, in which 'S' denotes a "special" design bar stress with confining steel. North Carolina State University (NCSU) ran duplicates of four beams tested at UT.

Table 2.1 - Matrix of test specimens from all schools

f'_c (ksi)	d_b (No.)	Cover (in.)	KU O**	KU X**	NCSU O	NCSU X	UT* O	UT* X
5	5	3/4	**0**	**0**			**0**	**0**
		$2d_b$	**0**	**0**			**0**	**0**
		$3d_b$					0	0
	8	1.5	**0**,1,**2**	**0**,1,**2**			**0**,**2**	**0**,**2**
		2.5			0,1,2	0,1,2		
	11	2			0,1,2	0,1,2		
		3					0,1,2	0,1,2
8	8	1.5			**0**,**2**	**0**,**2**	**0**,1,**2**	**0**,1,**2**
		2.5	0,1,2	0,1,2				
	11	2	0,1,2	0,1,2				
		3			0,1,2	0,1,2		
Total Specimens			22		22		22	

Confinement Levels

*Does not show UT specimens 8-5-SC0-1.5, 8-5-SC1-1.5, and 8-5-SC2-1.5

**ID representing the bar stress without confining transverse steel

Five series of specimens were tested at KU, as shown in Table 2.2. Series 1 and 2 are duplicates of beams tested at UT, while Series 3, 4, and 5 are complete sets of six. The series are split into groups according to splice length; 'A' denotes the shorter of the two splice lengths (and lower bar stress at splice failure), while 'B' is the longer (with the higher bar stress at splice failure).

Table 2.2 - Matrix of KU test specimens

Series	Group	Specimen	Bar Size	Nominal f'_c	Minimum Cover	Nominal Section	Splice Length	Design Stress
			(No.)	(ksi)	(in.)	(in. x in.)	(in.)	(ksi)
1	A	**5-5-OC0-3/4**	5	5	0.75	14 x 20	32	80
	B	**5-5-XC0-3/4**					43	100
2	A	**5-5-OC0-2d_b**			1.25	35 x 10	18	80
	B	**5-5-XC0-2d_b**					25	100
3	A	**8-5-OC0-1.5**	8	5	1.5	14 x 30	47	80
		8-5-OC1-1.5						100
		8-5-0C2-1.5						120
	B	**8-5-XC0-1.5**					63	100
		8-5-XC1-1.5						120
		8-5-XC2-1.5*						140
4	A	**8-8-OC0-2.5**		8	2.5	14 x 21	27	80
		8-8-OC1-2.5						100
		8-8-OC2-2.5						120
	B	**8-8-XC0-2.5**					36	100
		8-8-XC1-2.5						120
		8-8-XC2-2.5						140
5	A	**11-8-OC0-2**	11	8	2	24 x 26	58	80
		11-8-OC1-2						100
		11-8-OC2-2						120
	B	**11-8-XC0-2**					79	100
		11-8-XC1-2						120
		11-8-XC2-2**						140

*T-beam with b_f = 28 in. and h_f = 7 in.

**T-beam with b_f = 38 in. and h_f = 7 in.

2.2 Test Specimens

2.2.1 Flexural Design

The design methods described in this section were used for the specimens tested at KU, although the procedures were similar for all three universities. Table 2.3 summarizes the geometrical and reinforcement details of the twenty-two beam-splice specimens tested at KU.

Table 2.3 - Summary of flexural design details

Specimen		Design Beam Dimensions				Shear Reinforcement		Longitudinal Reinforcement				
Group	Designation	Support Spacing (ft)	Span, L (ft)	Effective Depth, d (in.)	Depth to A_s', d' (in.)	Bar Size (No.)	c/c Spacing, s_2 (in.)	Bar Size (No.)	No. of Bars (ea.)	Area of Tension Steel, A_s ($in.^2$)	Area of Compr. Steel, A_s ($in.^2$)	Target Bar Stress, f_s (ksi)
1A	5-5-OC0-3/4	7	15	18.94	1.81	4	4	5	4	1.76	1.76	80
1B	5-5-XC0-3/4	7	15	18.94	1.81	4	4	5	4	1.76	1.76	100
2A	5-5-OC0-2d_b	7	15	8.44	1.75	4	4	5	4	1.76	0.80	80
2B	5-5-XC0-2d_b	7	15	8.44	1.75	4	4	5	4	1.76	0.80	100
3A	8-5-OC0-1.5	10	21	28.00	1.75	4	4.5	8	2	1.58	0.40	80
	8-5-OC1-1.5	10	21	28.00	1.75	4	4.5	8	2	1.58	0.40	100
	8-5-OC2-1.5	10	21	28.00	1.75	4	4.5	8	2	1.58	0.40	120
3B	8-5-XC0-1.5	10	21	28.00	1.75	4	4.5	8	2	1.58	0.40	100
	8-5-XC1-1.5	10	21	28.00	1.75	4	4.5	8	2	1.58	0.40	120
	8-5-XC2-1.5	10	21	28.00	2.00	4	4.5	8	2	1.58	3.16	140
4A	8-8-OC0-2.5	10	21	18.00	2.00	4	5	8	2	1.58	1.58	80
	8-8-OC1-2.5	10	21	18.00	2.00	4	5	8	2	1.58	1.58	100
	8-8-OC2-2.5	10	21	18.00	2.00	4	5	8	2	1.58	1.58	120
4B	8-8-XC0-2.5	10	21	18.00	2.00	4	5	8	2	1.58	1.58	100
	8-8-XC1-2.5	10	21	18.00	2.00	4	5	8	2	1.58	1.58	120
	8-8-XC2-2.5	10	21	18.00	2.00	4	5	8	2	1.58	1.58	140
5A	11-8-OC0-2	11	24	23.50	1.75	5	4.5	11	2	3.12	0.40	80
	11-8-OC1-2	11	24	23.50	1.75	5	4.5	11	2	3.12	0.40	100
	11-8-OC2-2	11	24	23.50	1.75	5	4.5	11	2	3.12	0.40	120
5B	11-8-XC0-2	11	24	23.50	1.75	5	4.5	11	2	3.12	0.40	100
	11-8-XC1-2	11	24	23.50	1.75	5	4.5	11	2	3.12	0.40	120
	11-8-XC2-2	11	24	23.50	1.97	5	4.5	11	2	3.12	3.56	140

*Height of Series 1 specimens was 20 in. for the middle 6 ft. of the beam.

2.2.2 Shear Design

Shear reinforcement for the portions of the beams outside of the central constant moment region was designed in accordance with procedures outlined in ACI 318-05. The spacing of closed stirrups s_2 varied between 4 and 5 in. Series 1 through 4 used No. 4 closed stirrups as shear reinforcement, while Series 5 used No. 5 stirrups. The closed stirrups were made with Grade 60 ASTM A 615 steel and fabricated with 135º hooks at one corner. The majority of the stirrups used in the testing program and all of the stirrups used in specimens in Series 1 and 5 were bent at a fabricating shop; some of the stirrups used in Series 2, 3, and 4 were fabricated at KU.

2.2.3 Splice Design

Splice Length and Confinement

Test specimens were designed with lap splices centered at the midspan of the beam. Two splice lengths ℓ_s were selected for each series that, according to ACI 408R-03, would result in bond failure at bar stresses of 80 and 100 ksi if the splices were not confined by transverse reinforcement. These specimens were designated as "OC_" or "XC_", with "O" denoting the shorter splice length, and "X" the longer. Stirrups provided two levels of confinement, "_C1" and "_C2", designed to increase the bar stress at failure for each splice length by 20 or 40 ksi, respectively. The nominal center-to-center spacing between transverse reinforcement over the length of the splice s_1 is listed in Table 2.4. The resulting nominal splice strengths are 80, 100, and 120 ksi for specimens OC0, OC1, and OC2, respectively, and 100, 120, and 140 ksi for specimens XC0, XC1, and XC2.

Concrete Cover

Test specimens containing No. 8 and No. 11 bars were designed to have equal amounts of concrete clear cover on the bottom c_b and sides c_{so} of the spliced bars to help ensure an equal likelihood of failure by bottom or side splitting. The No. 8 bars had a clear spacing $2c_{si}$ equal to twice the concrete clear cover, while the No. 11 bars had a clear spacing greater than two times the clear cover. Specimens containing No. 5 bars were designed as slabs and, thus, had clear bar spacings that were greater than twice the bottom cover to simulate typical slab construction. Clear spacing remained twice the side cover. Figure 2.2 shows the typical cross-sectional layouts for all beam splice-specimens.

Table 2.4 - Splice and cover dimensions for KU specimens

Specimen		Splice Design								
Group	Designation	Splice Length, l_s (in.)	Bottom cover, c_b (in.)	Outside cover, c_{so} (in.)	Half clear spacing c_{si} (in.)	No. 4 Stirrups (ea.)	c/c Tie Spacing, s_1 (in.)	Bar Size (No.)	No. of Bars (ea.)	Target Bar Stress, f_s (ksi)
1A	5-5-OC0-3/4	32	0.75	1.13	1.13	--	--	5	4	80
1B	5-5-XC0-3/4	43	0.75	1.13	1.13	--	--	5	4	100
2A	5-5-OC0-2d_b	18	1.25	3.75	3.75	--	--	5	4	80
2B	5-5-XC0-2d_b	25	1.25	3.75	3.75	--	--	5	4	100
3A	8-5-OC0-1.5	47	1.5	1.5	3.5	--	---	8	2	80
	8-5-OC1-1.5	47	1.5	1.5	3.5	4	11 3/4	8	2	100
	8-5-OC2-1.5	47	1.5	1.5	3.5	8	5 7/8	8	2	120
3B	8-5-XC0-1.5	63	1.5	1.5	3.5	--	--	8	2	100
	8-5-XC1-1.5	63	1.5	1.5	3.5	4	15 3/4	8	2	120
	8-5-XC2-1.5	63	1.5	1.5	3.5	8	7 7/8	8	2	140
4A	8-8-OC0-2.5	27	2.5	2.5	2.5	--	--	8	2	80
	8-8-OC1-2.5	27	2.5	2.5	2.5	2	13 4/8	8	2	100
	8-8-OC2-2.5	27	2.5	2.5	2.5	5	5 3/8	8	2	120
4B	8-8-XC0-2.5	36	2.5	2.5	2.5	--	--	8	2	100
	8-8-XC1-2.5	36	2.5	2.5	2.5	2	18	8	2	120
	8-8-XC2-2.5	36	2.5	2.5	2.5	5	7 1/4	8	2	140
5A	11-8-OC0-2	58	2	2	7.18	--	--	11	2	80
	11-8-OC1-2	58	2	2	7.18	4	14 1/2	11	2	100
	11-8-OC2-2	58	2	2	7.18	9	6 1/2	11	2	120
5B	11-8-XC0-2	79	2	2	7.18	--	--	11	2	100
	11-8-XC1-2	79	2	2	7.18	4	19 3/4	11	2	120
	11-8-XC2-2	79	2	2	7.18	9	8 3/4	11	2	140

*Height of Series 1 specimens was 20 in. for the middle 6 ft. of the beam.

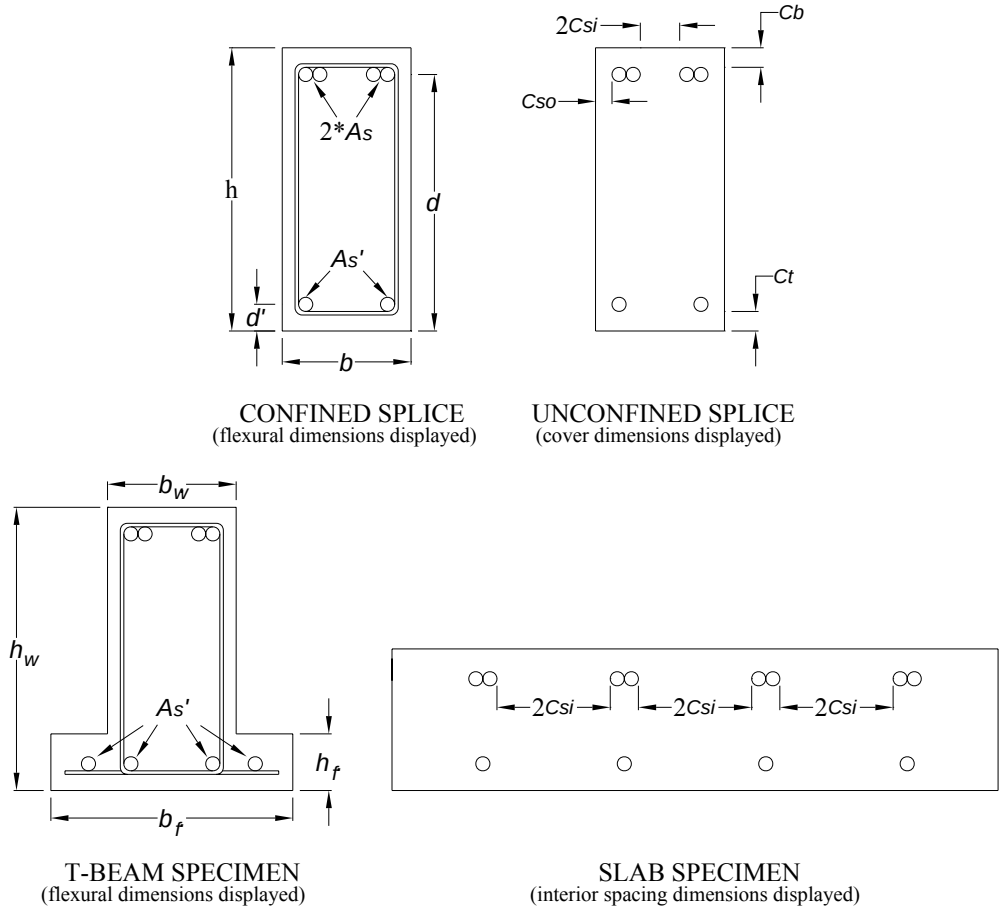

Figure 2.2 - Cross sections of all specimen types, as tested

2.2.4 T-beam Design

Early in the testing program, specimen 8-5-XC2-1.5 failed in flexure in the compression region near the support. As a result, both that specimen and 11-8-XC2-2, which were designed to reach stresses of 140 ksi at splice failure, were redesigned as T-beams with larger amounts of compression steel to increase their flexural capacity and avoid flexural failures. Specimen 8-8-XC2-2.5, the other beam tested at KU with a predicted bar stress of 140 ksi, had already been cast and failed in bond in

the splice region and therefore did not have to be redesigned. The flanges on both specimens were 14 in. wider than the original web width and 7 in. deep. Additional compression reinforcement, consisting of four No. 8 bars, was used for both beams. All other properties of the beams remained unchanged.

2.2.5 Span Length

The nearly constant moment resulting from four-point loading eliminates the effects of shear forces in the splice region and therefore the need for shear reinforcement in the middle portion of the beam, allowing transverse reinforcement to be used solely as confinement for the splices.

All specimens were designed so that the support spacing ensured a distance from either end of the splice to the central pin and roller supports equal to or greater than the effective depth of the beam *d*. The loading span lengths were selected to induce moments causing bar stresses of 150 ksi at moderate loads. The span lengths were selected in increments of three feet based on the available 3-ft spacing of load points in KU's structural testing laboratory. The specimens were inverted for testing, as shown in Figures 2.2 and 2.3.

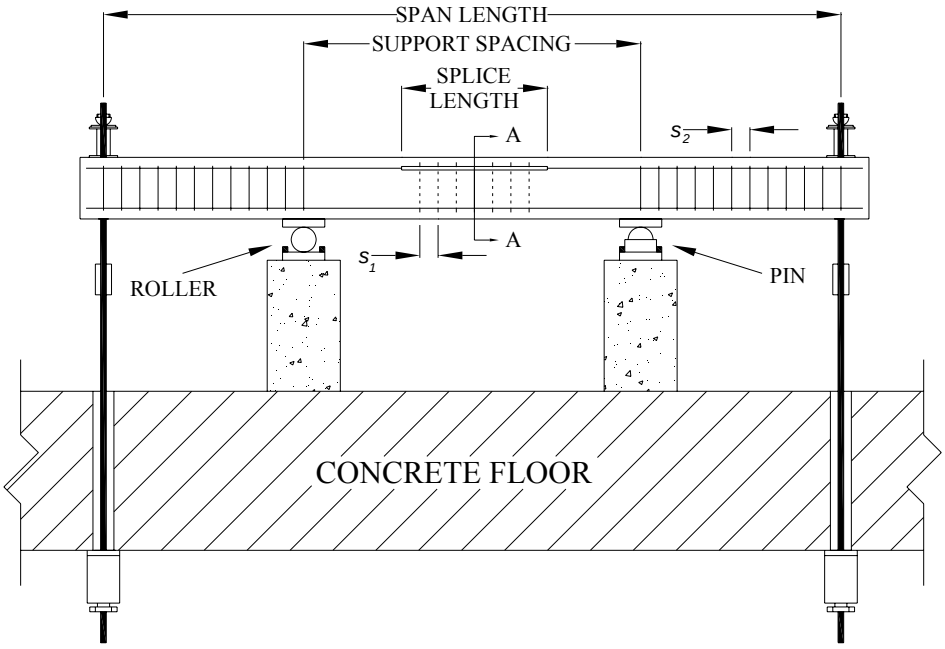

Figure 2.3 - Elevation view of the test setup

2.3 Materials

2.3.1 Tension Steel

The longitudinal tension reinforcement in the specimens was Grade 100 reinforcing steel. The stress-strain relationship used for the Grade 100 steel for flexural design was that proposed by Dawood et. al. (2004), shown in Eq. (2.1).

$$f_s = 165(1 - e^{-185\varepsilon_s}) \tag{2.1}$$

where:

f_s = stress in the steel (ksi)

ε_s = strain in the steel

The specimens in Series 1 and 2 were designed to simulate slabs, and contained four No. 5 bars as tension reinforcement. Specimens in Series 3 and 4

contained two No. 8 bars, while those in Series 5 used two No. 11 bars as primary reinforcement.

2.3.2 Compression Steel

All specimens contained longitudinal bars in the compression region to anchor the stirrups used as shear reinforcement and the confining transverse reinforcement. The specimens in Series 1 and 4 were designed using compression steel to provide adequate flexural capacity for the beam, while all other designs ignored the presence of top steel because the bars were small and not required to provide flexural strength. Specimens in Series 1 and Series 2 contained four No. 5 bars and four No. 4 bars, respectively. Specimens in Series 4 used two No. 8 bars, while specimens in both Series 3 and 5 used two No. 4 bars. All compression steel consisted of standard Grade 60 ASTM A 615 steel and was assumed to follow a bi-linear stress-strain curve as described by Eq. (2.2).

$$f_s = 29000 \times \varepsilon_s \leq 60 \text{ ksi} \tag{2.2}$$

2.3.3 Concrete

Target concrete compressive strengths of 5 and 8 ksi were selected to represent concrete strengths found in actual construction because mixes with specified strengths of 4 and 6.5 ksi often reach 5 and 8 ksi, respectively. All specimens were cast with normalweight, non-air-entrained concrete consisting of Ash Grove Type I/II portland cement, water, Kansas River sand, and crushed limestone coarse aggregate with a maximum aggregate size of ¾ in. High-range water reducing admixtures (HRWRAs) were used in all 8 ksi mixes and as needed in 5 ksi mixes to meet workability targets. Concrete mix design details are presented in Appendix A.

2.4 Specimen Manufacture

2.4.1 Reinforcing Cage

The beam specimens were constructed one foot longer than the design loading span to accommodate the loading apparatus. Longitudinal reinforcement was terminated one inch from the end of the specimen to allow for construction tolerances. Shear reinforcement was continued to the end of the longitudinal reinforcement.

Grade markings were allowed within the splice region. The grade markings did not interrupt the typical deformation pattern for either the No. 8 or No. 11 bars, and while deformations were removed on the No. 5 bars to accommodate the grade stamp, the markings were staggered with such frequency that some portion of a grade marking would remain within the splice length on every specimen.

The cages were assembled using standard 8 in. and 10 in. wire ties. The reinforcement was cut with a band saw, and band saw cut ends of tension reinforcement were used within the splices to avoid inconsistencies in material properties and bar geometry common to the shear-cut ends of the as-delivered bars.

Transverse anchor bars were welded within 2 in. of the end of the longitudinal reinforcement on all specimens, except those in two of the earliest test specimens, 8-5-OC0-1.5 and 8-5-XC0-1.5. An early specimen not included in this report exhibited bond failure near the loading apparatus at one end of the beam, precipitating a shear failure in that specimen. The anchor bars used in subsequent specimens provided additional bearing area to ensure proper bar development at the termination of longitudinal steel. The bond failure precipitated a shear failure in that specimen. Additionally, the welded anchor bars kept the cage square and rigid during transport.

Cover tolerances were achieved using standard steel reinforcement chairs attached directly to the longitudinal bars, a stirrup, or to a short piece of reinforcing bar of the size needed to maintain the appropriate cover of the supported longitudinal bar.

2.4.2 Formwork

Specimens were cast in individual forms constructed of ¾-in. plywood and 2x4s. The forms were protected using a multiple-layer polyurethane coating, and mineral oil was used as a release agent for all surfaces exposed to concrete. ⅜-in. all-thread low carbon steel rods were used in all specimens, with the exception of the two slab-beams in Series 2, to maintain correct width and transfer lateral force from the weight of the concrete to the form stringers. The rods passed through the specimen approximately 6 in. from the compression face of the beam at a spacing of 2 ft center-to-center throughout the entire length of the beam and remained in the concrete during the splice tests.

Because the test apparatus required the load rods be spaced at 36 in. transversely at the ends of the span, specimens in Series 2 and specimen 11-8-XC2-2, a T-beam, required blockouts to reduce the section width at the loading points to accommodate the load rods. Descriptions of the reduced section are found in the specimen details located in Appendix B. No longitudinal bars were terminated due to these changes, and adequate cover was maintained for all longitudinal steel.

2.4.3 Concrete Placement and Curing

The beams were cast using ready mix concrete. In most cases, they were cast in pairs. Workability was adjusted as needed by adding water that had been withheld during batching or by adding a high-range water reducer. Due to variability between concrete loads, all specimens using a specific mix design were not cast with identical batch quantities, although all 5 ksi and 8 ksi beams were each cast using the same two nominal mix designs, which may be found in Appendix A.

The beams were cast in two layers, beginning and ending at the ends of the beams, while placing the bottom and top layers of concrete in the splice regions of both beams from the middle portion of the batch to help ensure placement of the best quality concrete in the splice region. Concrete samples for strength specimens and standard concrete tests were taken in accordance with ASTM C 172 immediately before and after placing the first lift in both of the splice regions and were combined

prior to testing the plastic concrete and casting the strength specimens. The concrete in the beams was consolidated using internal vibration after a complete layer had been placed.

After casting, beams were typically cured in the forms and covered with wet burlap and plastic sheeting on the exposed face until approximately three-quarters of the desired compressive strength had been reached, at which point the forms were stripped and the beams set on blocks to air-dry on all faces. Some specimens were stripped prior to attaining three-quarters of the final strength and were instead completely covered in wet burlap and wrapped in plastic sheeting. During moist curing, beams were rewet a minimum of once per day.

2.4.4 Strength Specimens

Standard 6 × 12 in. concrete cylinders were cast in accordance with ASTM C 192 along with the splice specimens. The cylinders were stored next to the beams as they cured, and were stripped simultaneously with the beams.

Cylinders cast in disposable plastic molds were used to track the strength of the concrete as the beams cured. Three cylinders per beam were cast in steel molds; these cylinders were used to establish the concrete compressive strength when the beams were tested. The cylinders were capped in accordance with ASTM C 617 before testing. The cylinders were tested immediately after the completion of the splice test, and strengths recorded to the nearest 10 psi, in accordance with ASTM C 39. Generally, if multiple beams were tested within a 24-hour period, the compressive strength of two beams cast simultaneously was treated as the same, and all cylinder strengths were averaged.

2.4.5 Measurements

Section Properties

The beams were marked to indicate the locations of the load apparatus, pin and roller supports, ends of the splice region, and the beam centerline. All longitudinal measurements were taken from the centerline of the beam to eliminate

any inconsistencies for beams slightly longer or shorter than the nominal length. The markings were 'PS' for the pedestal support, 'SR' to indicate the end of the splice region, and 'CL' for the centerline of the beam. The beams were also marked with cardinal directions for reference in photographs.

Beam width, height, and length were measured along the external faces of each specimen before testing. Height and width measurements were taken at 11 locations along all sides of each beam, including the pin and roller support locations, both ends of the splice region, and the centerline of the beam. Total beam length was typically measured on each side of the beam on both the compression and tension faces. To ensure accurate measurements, any excess concrete or surface variations were removed from corners of the beams with an abrasive block or angle grinder. Measurements were taken to $^{1}/_{32}$-in. accuracy.

Cover

Because of the inaccuracies inherent to measuring cover prior to casting, clear cover values are based on post-break measurements obtained from concrete debris broken at splice failure or with an air chisel after the completion of testing. Measurements were taken at each end of the splice because the moment is assumed to be highest there due to the self-weight of the beam. Concrete was also removed to expose the compression reinforcement in these locations.

Clear cover measurements taken at each splice end (based on original orientation at casting) include bottom cover to the tension reinforcement, external side cover, and top cover to the compression reinforcement. Additionally, the internal clear spacing between splices was measured. Measurements to the tension reinforcement were made to the bar deformations, whereas the top cover was measured to the solid bar stock. All concrete cover measurements were made with calipers accurate to 0.001 in.

Bar deformation properties

The bar deformation characteristics were measured and the relative rib areas calculated for the Grade 100 ASTM A 1035 bars used in this study. Relative rib area is a measure of the bearing area of deformations on a reinforcing bar normalized to the surface area of that bar between deformations. Relative rib area was measured in accordance with ACI 408.3-01/408.3R-01 (ACI Committee 408 2001).

Six-inch digital calipers were used to determine the average width and spacing of the deformations. A knife-edge dial gage spanning two deformations was used to determine the deformation height in five places between the ribs. All measurements were taken on a minimum of five deformations per bar to ensure consistency. Measurements were accurate to 0.001 in. The relative rib areas were determined to be 0.0767 for No. 5 bars, 0.0838 for No. 8 bars, and 0.0797 for No. 11 bars. The three bars are shown in Figure 2.4. Further details may be found in Table A.4 in Appendix A.

Figure 2.4 - Photograph of No. 5, No. 8, and No. 11 Grade 100 reinforcing steel

2.4.6 Test Setup

All specimens were designed to be tested in four-point bending. Prior to testing, each beam was inverted from its casting position. This was done by rotating

the beams while they were supported on longitudinal No. 8 bars cast into and projecting out of the ends of the beams. The beams were initially cast tension-face down to avoid any top-bar effect on the primary reinforcement, which is known to reduce bond strength of reinforcing bars. They were tested in an inverted position for safety and ease of marking cracks.

As shown in Figure 2.5, the two central reactions were provided by pin and roller supports made of cold-worked, solid round-stock steel bars in contact with the compression face through 1-in. thick cold-rolled bearing plates. The pin and roller were mounted on concrete pedestals that were, in turn, supported by a 2-ft thick reinforced concrete structural floor. All surfaces involved in load transfer were covered with a layer of Hydrostone, a 10,000 psi high strength gypsum plaster, which is used to prevent movement between the surfaces and ensure even load distribution.

Beams in Series 3 and 4 were supported by a 6-in. diameter roller and pin, both 12 in. long, with appropriately sized bearing plates above and below, with the exception of specimen 8-5-XC2-1.5, a T-beam. All other beams, including both T-beams, were supported on 30-in. long, 2⅝-in. diameter round-stock, on 30 x 6-in. bearing plates. Pin supports were fabricated by welding the round-stock to the lower bearing plate, allowing no translation between the two.

At each end of the beam, loads were applied through a W8x48 steel spreader beam spanning the tension face. Each spreader beam was connected to two 1½-in. diameter high-yield threaded rods which were passed through stiffened openings in the wide flange section. These rods were pulled downward through the structural concrete floor by load-equalized hydraulic jacks connected to a central pump. Load cells on each of the four load rods were independently calibrated from 0 to 100 kips, approximately twice the highest load on a single rod required for any test.

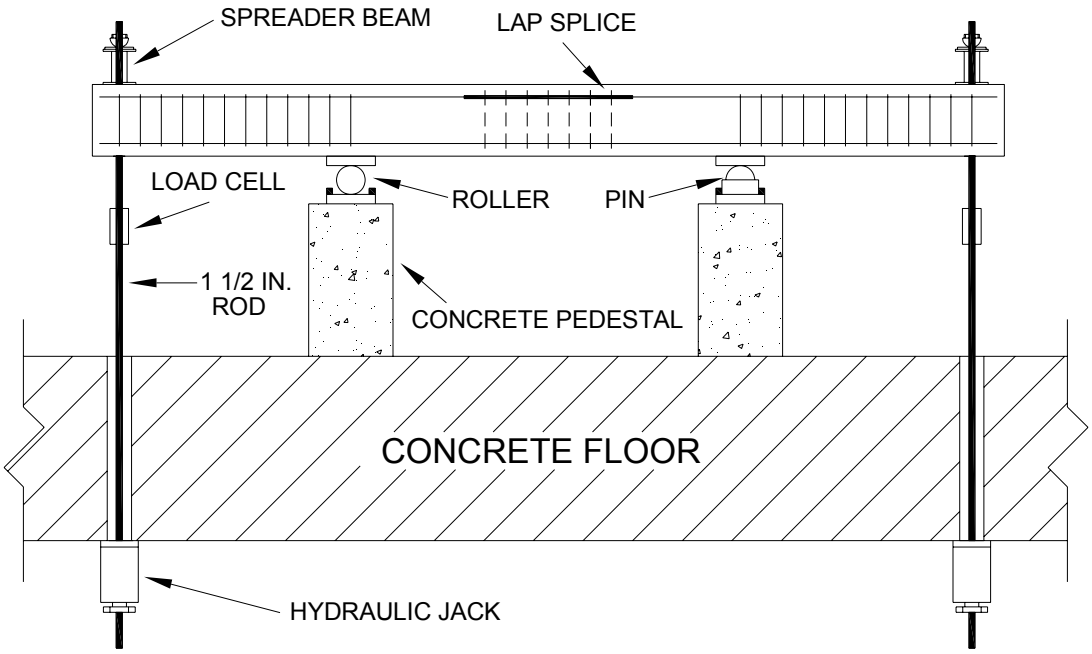

Figure 2.5 - Schematic of the test setup

2.4.7 Instrumentation

Three linear variable differential transformers (LVDTs) were used to record the vertical beam deflections; one at midspan and one at each load application point at the end of the span. A dial gage was attached to each LVDT stand so that beam deflections could also be recorded by hand. The applied load was measured using load cells located on each rod consisting of a group of four strain gages arranged in a full Wheatstone bridge. Readings from the LVDTs and load cells were monitored and recorded using a data acquisition (DA) system. The DA system recorded readings from the LVDTs and the load cells at a rate of 4 Hz.

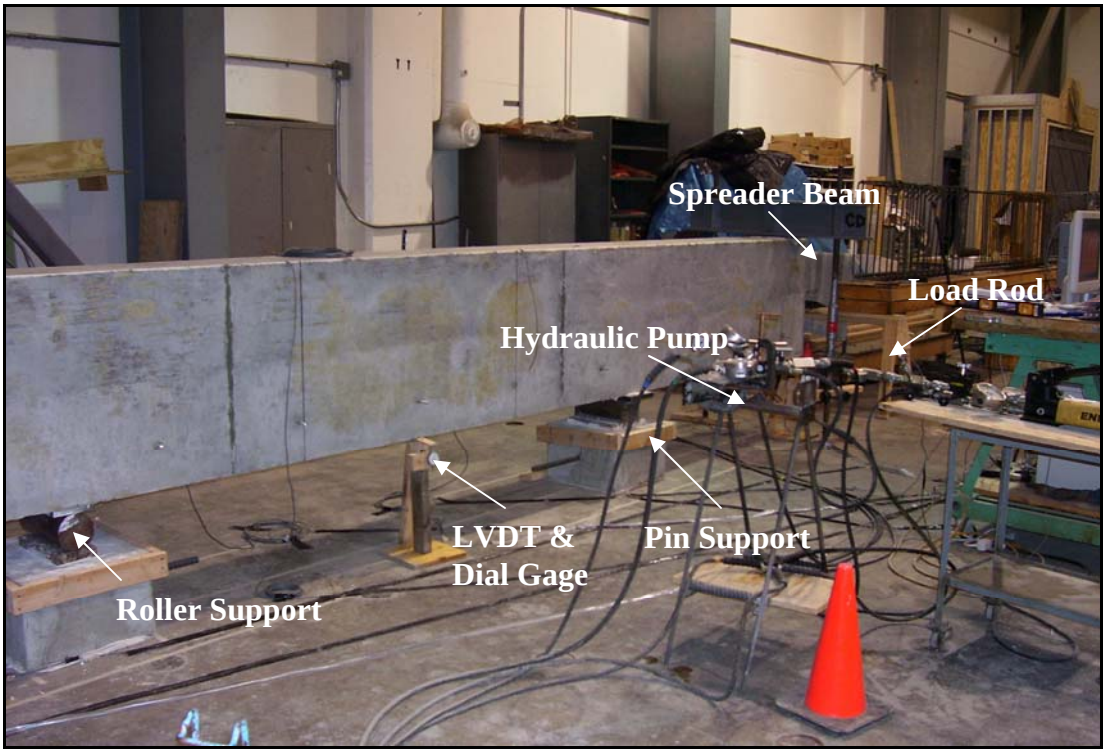

Figure 2.6 - Photograph of the test setup

Within each specimen, four 120Ω ¼-in. strain gages with attached leads were bonded to the primary tension reinforcement. One strain gage was placed on each spliced bar approximately two inches outside the end of the splice. One deformation on each No. 8 and No. 11 bar was removed using low-heat grinding and polishing to provide a level surface for attaching the strain gage. No. 5 bars typically required the removal of two deformations. Strain gages were applied and sealed following the manufacturer's recommended procedures for submersion in concrete. The coating used to seal the strain gages typically covered a number of deformations, all outside of the splice region. Strain gages were read using strain indicator boxes.

2.5 Test Procedure

Prior to each test, the double acting jack system was pumped fully in reverse, after which all slack was taken out of the load rods by tightening the nuts until each load rod was almost engaged with the fully retracted hydraulic jacks. This was done

to ensure even loading across all four rods. After zeroing all LVDT, load cell, and strain gage readings on the DA system and strain indicator boxes, zero readings were recorded for each of the three dial gages. Load was applied using a manually-controlled hydraulic pump. Pauses were incorporated in the loading sequence at predetermined load levels to visually inspect the beam, mark visible cracks, measure crack widths using crack comparators, and to record strain and dial gage readings.

The initial load increment was always half of the estimated cracking load to ensure that all instruments and the hydraulic system were operating properly, while the second load step reached the estimated cracking load. The total number and size of load increments varied depending on the estimated capacity of the specimen being tested. Pauses typically were limited to 4 minutes or less. Following specimen failure, the jacks were pumped in reverse until all load was removed from the rods and the jacks were fully retracted.

Due to the brittle nature and large amount of stored energy released in splice failures, the final load step at which cracks were marked and measured was typically set as ⅔ of the estimated failure load. After this point, the load was increased steadily until failure.

2.6 Section Analysis

2.6.1 General

Loads, moments, and stresses for the beams were calculated using a two-dimensional analysis in which loads and reactions were assumed to act along the longitudinal centerline of the beam. Reactions and moments were based on load cell readings and the weight of the loading assemblies. The self-weight of the beam was included in the calculations based on average beam dimensions and an assumed density of 150 pcf. Given that specimens generally experienced nearly identical moments at both ends of the splices, splitting failures were assumed to initiate from the splice end with the smallest measured cover dimension.

The test specimens were evaluated using a cracked section analysis with a linear strain distribution throughout the cross-section. The beams were analyzed by both strength and moment-curvature methods for comparison. The moment-curvature method uses a nonlinear stress-strain curve for the concrete, while the strength method uses an equivalent stress block. Good agreement in calculated values was noted between the two methods, and most of the comparisons that follow will be based on the moment-curvature method. It should be noted that bar stresses based on the moment-curvature method slightly exceeded those obtained using the strength method. Figure 2.7, modified from Nawy (2003), is a representation of the moment-curvature and strength methods of section analysis.

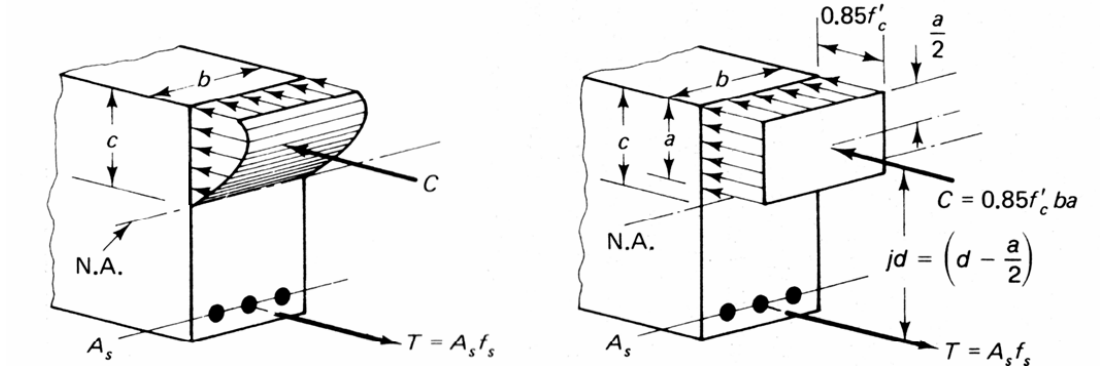

Figure 2.7 - Moment-curvature and strength analysis [after Nawy (2003)]

2.6.2 Reinforcing Steel

The steel tensile stress f_s (ksi) of MMFX Grade 100 reinforcing steel was estimated using the stress-strain curves given in Eq. (2.3) and (2.4) and provided by UT (Glass 2007). Equation 2.3 was used for both No. 5 and 8 bars, while Eq. (2.4) was used for No. 11 bars. The compression steel is standard Grade 60 steel and is assumed to follow the bi-linear stress-strain curve given in Eq. (2.5). Figure 1.2 shows the steel stress-strain curves.

$$f_s = 156 \times \left(1 - e^{-220\varepsilon_s}\right) \tag{2.3}$$

$$f_s = 162 \times (1 - e^{-235\varepsilon_s}) \tag{2.4}$$

$$f_s = 29000 \times \varepsilon_s \leq 60 \text{ ksi} \tag{2.5}$$

Concrete

Evaluations made with the strength method used the Whitney stress block and the values of β_1 provided in ACI 318-05. Concrete stress f_c and strain ε_c in the moment-curvature calculations were estimated using the modified concrete stress-strain relationship developed by Hognestad (1951). Both analyses neglect the tensile strength of the concrete. The modified Hognestad relationship is listed as Eq. (2.6). Figure 2.8 shows stress-strain curves for 5 and 8 ksi concrete.

$$f_c = \begin{cases} f_c'' \left[2\left(\dfrac{\varepsilon_c}{\varepsilon_0}\right) - \left(\dfrac{\varepsilon_c}{\varepsilon_0}\right)^2 \right] & \text{for} \quad \varepsilon_c \leq \varepsilon_0 \\ f_c'' \left[0.15\left(\dfrac{\varepsilon_0 - \varepsilon_c}{\varepsilon_{cu} - \varepsilon_0}\right) + 1 \right] & \text{for} \quad \varepsilon_c \geq \varepsilon_0 \end{cases} \tag{2.6}$$

$$f_c'' = 0.85 f_c' \tag{2.7}$$

$$\varepsilon_0 = \frac{1.7 f_c'}{E_c} \tag{2.8}$$

$$E_c = 1.8 \times 10^6 + 460 f_c' \tag{2.9}$$

where:

f_c = concrete stress

f_c' = concrete compressive strength

f_c'' = peak concrete stress

ε_c = concrete strain

ε_0 = concrete strain at peak stress

ε_{cu} = ultimate concrete strain at crushing = 0.0038

E_c = approximate concrete modulus of elasticity

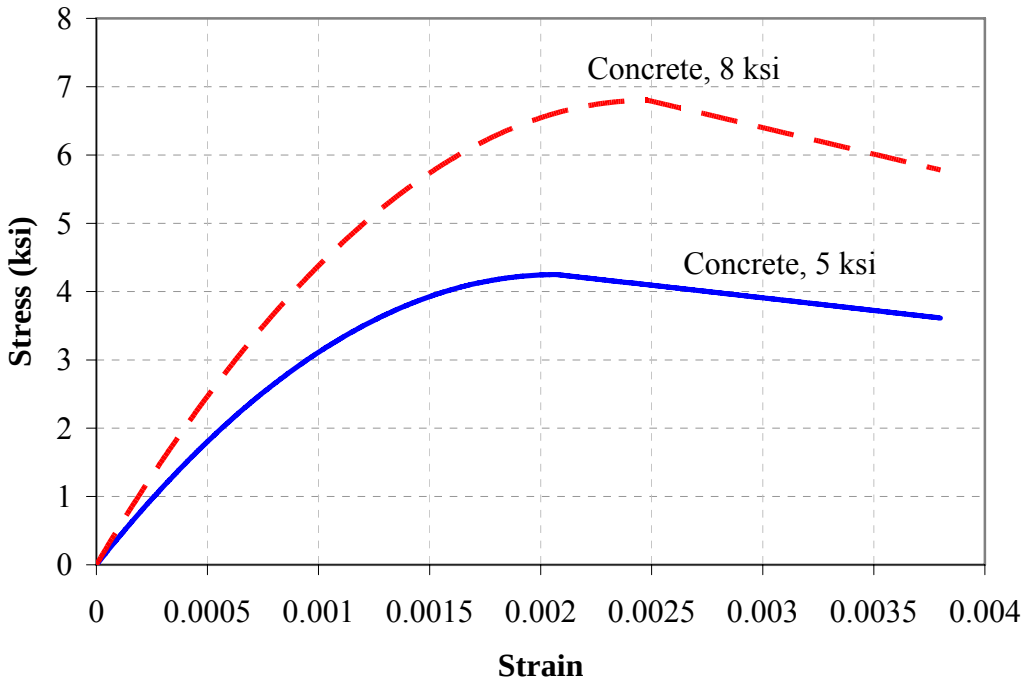

Figure 2.8 - Hognestad Stress-strain curves

CHAPTER 3

RESULTS AND EVALUATION

3.1 General

The twenty-two beam splice specimens tested at KU were evaluated with respect to observed failure mode, load-deflection behavior, comparison of the calculated bar stresses versus the predicted bar stresses, and crack patterns. Reported here are results for the 64 specimens that failed in bond at all schools, as well as more detailed results for the 22 specimens tested at KU. Table 3.1 summarizes the concrete strength, cover and spacing measurements, splice lengths, quantity of confining transverse reinforcement, and the bar stresses at failure, as predicted by ACI 408R-03 and calculated based on the strength or moment-curvature method for the test specimens for the KU specimens. Additional details regarding the KU specimens may be found in Appendix B.

Table 3.1 - Summary of KU specimen results

Group	Specimen	Bar Size	f'_c	c_b	c_{so}	c_{si}	Splice Length, l_s	Stirrups Confining Splice	Predicted Failure Stress (ACI 408R)	Actual Failure Stress	
										Strength	Moment Curvature
		(No.)	(psi)	(in.)	(in.)	(in.)	(in.)	(ea.)	(ksi)	(ksi)	(ksi)
1A	**5-5-OC0-3/4**	5	5,490	0.73	1.08	1.02	32	0	80.3	73.9	77.0
1B	**5-5-XC0-3/4**		4,670	0.66	0.92	1.09	43	0	90.7	79.5	82.2
2A	**5-5-OC0-2db**		5,490	1.05	3.72	3.67	18	0	77.4	83.1	86.9
2B	**5-5-XC0-2db**		4,670	0.98	3.80	3.64	25	0	89.8	87.8	91.2
3A	**8-5-OC0-1.5**	8	5,260	1.34	1.41	3.63	47	0	77.0	75.1	78.1
	8-5-OC1-1.5		4,720	1.54	1.51	3.32		4	99.5	122.1	123.5
	8-5-OC2-1.5		6,050	1.34	1.44	3.37		8	127.3	125.4	127.3
3B	**8-5-XC0-1.5**		5,940	1.35	1.41	3.62	63	0	99.5	87.0	90.0
	8-5-XC1-1.5		4,720	1.46	1.52	3.36		4	117.9	127.5	128.7
	8-5-XC2-1.5		5,010	1.30	1.53	3.23		8	135.5	141.4	143.0
4A	**8-8-OC0-2.5**		8,660	2.25	2.25	2.64	27	0	77.7	75.9	79.5
	8-8-OC1-2.5		7,790	2.37	2.19	2.54		2	89.5	85.3	88.7
	8-8-OC2-2.5		7,990	2.16	2.28	2.63		5	100.7	112.3	115.0
4B	**8-8-XC0-2.5**		7,990	2.32	2.38	2.61	36	0	96.1	87.7	91.1
	8-8-XC1-2.5		7,790	2.46	2.35	2.48		2	110.9	108.1	111.0
	8-8-XC2-2.5		8,660	2.25	2.44	2.57		5	129.3	114.5	117.4
5A	**11-8-OC0-2**	11	9,370	1.82	1.83	6.89	58	0	78.9	64.5	67.9
	11-8-OC1-2		9,370	1.55	1.68	7.25		4	94.6	91.7	95.5
	11-8-OC2-2		8,680	1.82	1.94	6.95		9	122.4	120.3	123.5
5B	**11-8-XC0-2**		9,910	1.76	1.87	7.30	79	0	99.1	75.2	78.9
	11-8-XC1-2		9,910	1.94	2.02	6.98		4	126.2	103.2	106.9
	11-8-XC2-2		8,680	1.71	2.12	6.88		9	140.6	134.4	137.3

.

3.1.1 Unconfined Splice Specimens

Beams without confining transverse reinforcement typically exhibited characteristics of a brittle failure and abruptly lost all load-carrying capacity. During testing, it was observed that the greater the failure load and likewise the stored energy, the greater the likelihood that the splices would fail explosively.

Specimens with low total loads and lower concrete strength also exhibited brittle splice failures, but were much less likely to fail in an explosive manner. During testing, it was observed that the exterior two (of four) splices in beams 5-5-OC0-2d_b and 5-5-XC0-2d_b failed or slipped prior to failure of the specimen. These two specimens were slab beams with four splices apiece and no confining transverse reinforcement. After initial failure of the exterior splices, the load dropped slightly,

but the beams carried further load until the inner splices failed. The peak loads are used for analysis.

3.1.2 Confined Splice Specimens

Beams with confining transverse reinforcement in the splice region typically failed more gradually and exhibited far greater ductility than beams without confining transverse reinforcement. Beams with confining transverse reinforcement consistently developed larger splitting cracks before failure and often could be heard cracking well before failure. Although failure was still brittle for beams with confined splices, the large increase in ductility provided by the transverse reinforcement is desirable.

3.2 Load-Deflection Behavior

The load-deflection behavior for each group of specimens was examined to evaluate the effect of splice strength and confining transverse reinforcement on the deformation capacity of the specimens. For all load-deflection plots, the total deflection of the beam is plotted versus the total load. As can be observed in the load-deflection behavior of the specimens in Group 3B, displayed in Figure 3.1, adding confining transverse reinforcement not only increases the splice strength but also deformation capacity. The additional load capacity and ductility are directly related to the quantity of confining transverse reinforcement. Specimens without confining transverse reinforcement failed in a brittle manner at significantly lower bar stresses and smaller overall beam deflections than those with confinement, while additional confinement further increased the bar stress and beam deflection before failure.

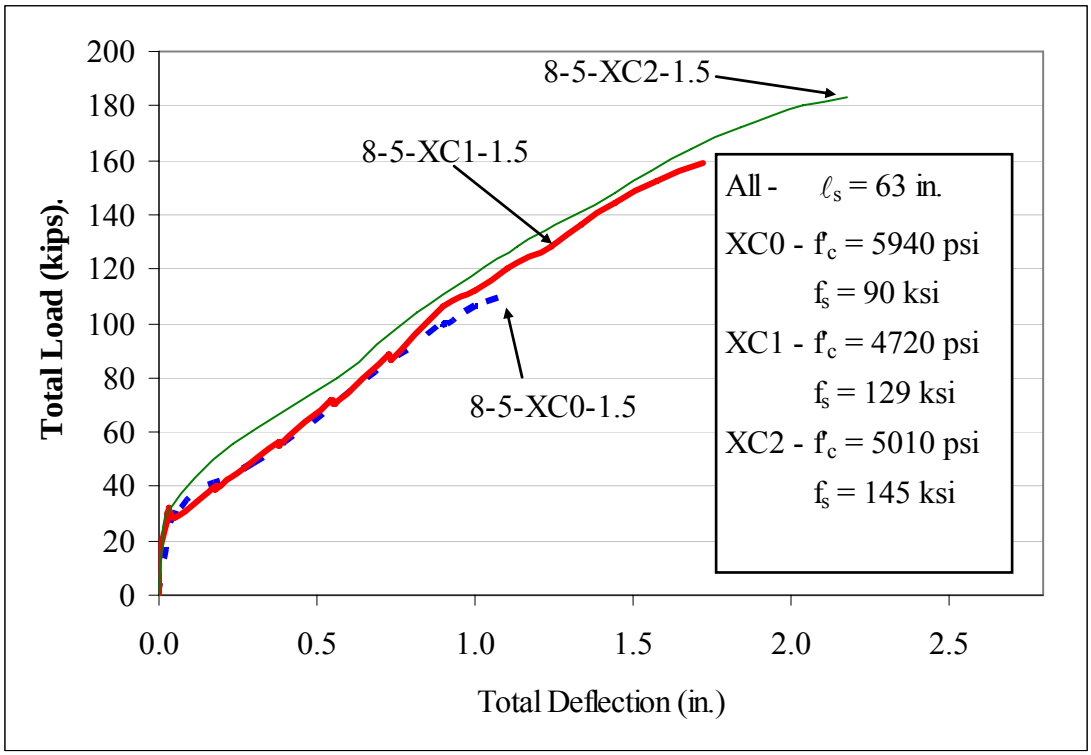

Figure 3.1 - Load-deflection behavior of Group 3B specimens

3.3 Calculated and Measured Bar Stresses

The calculations and comparisons made in this study are based on bar stresses calculated using the moment-curvature method. To determine the effects of reinforced concrete behavior not included in the assumptions of the moment-curvature method, most notably bar slip, four strain gages were applied to the primary tension bars immediately outside of the splices in each specimen as a means to measure actual bar stress. The measured bar stress is compared to the calculated bar stress at or near failure for Series 5 in Table 3.2. The measured bar stress is calculated based upon the measured strain and the same stress-strain curve as used for the moment-curvature calculations. As can be seen, the measured stresses closely correlate to the calculated stresses. The measured stresses are, on average, 1.5% higher than the calculated stresses, and range from 4% lower to 6% higher.

Table 3.2 - Measured versus calculated stresses for Series 5 specimens

Beam ID	Load (kips)	Calculated Stress* (ksi)	Measured Stress** (ksi)	Meas.-to-Calc. Difference (ksi)	Meas.-to-Calc. Difference (%)
11-8-OC0-2	117	68	71	2.7	4.0%
11-8-XC0-2	136	79	83	4.4	5.6%
11-8-OC1-2	168	95	99	3.4	3.5%
11-8-XC1-2	185	107	104	-3.0	-2.8%
11-8-OC2-2	212	124	123	-0.1	-0.1%
11-8-XC2-2	242	137	137	-0.3	-0.2%

* Based on moment-curvature method

** Based on measured strain and assumed stress-strain curve for MMFX steel in Eq. (2.4)

The stresses based on the strain gage data for Groups 5A and 5B are shown in Figures 3.2 and 3.3, respectively. A single representative strain gage from each test is shown in these graphs. It should be noted that specimen 11-8-OC2-2 (Figure 3.2) was loaded to a total load of roughly 48 kips, unloaded, and then reloaded due to technical problems with the hydraulic system. The graph shows only the reloading and, thus, does not display the behavior prior to cracking, indicated in all other records by the much shallower slope at low load levels. The final failure data points, indicated by asterisks, are calculated from moment curvature and included for comparative purposes.

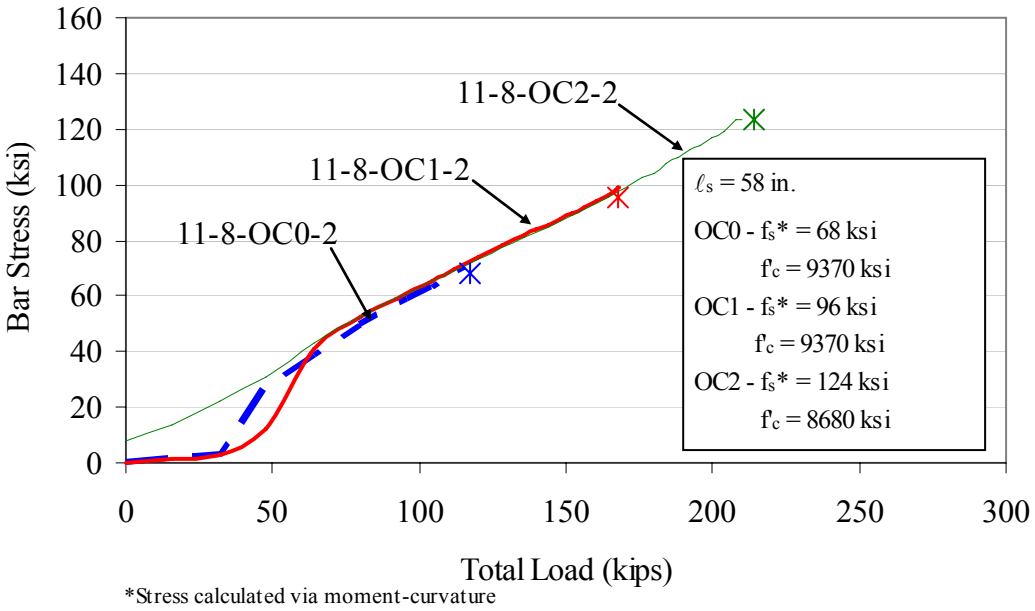

Figure 3.2 - Measured bar stress versus total load for Group 5A specimens

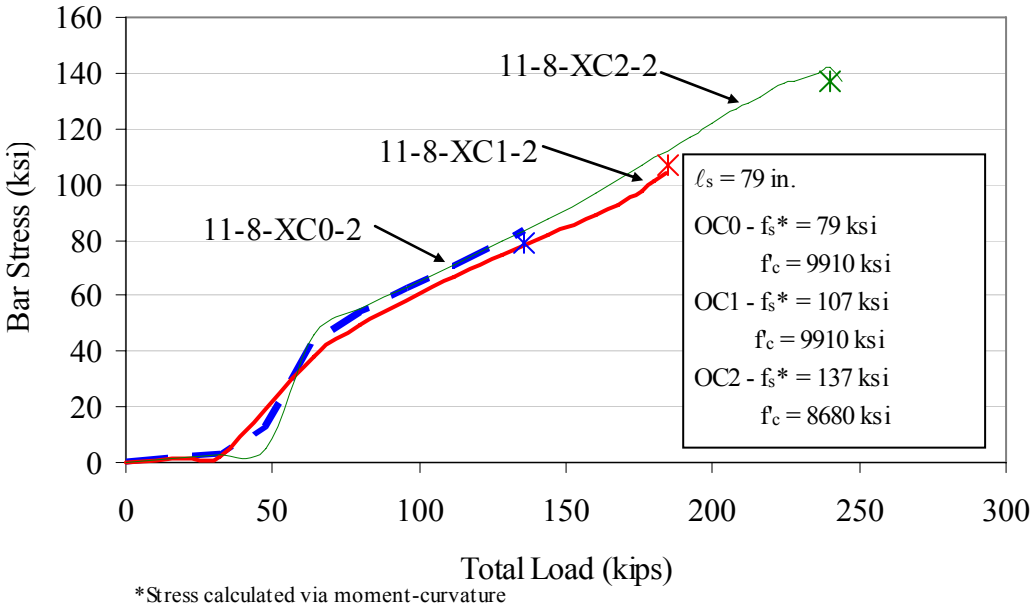

Figure 3.3 - Measured bar stress versus total load for Group 5B specimens

3.4 Cracking

During testing, flexural, splitting, and shear cracks formed in the specimens. Flexural cracks were observed first, while shear cracks and bond splitting cracks developed as loading continued. Crack patterns typically grew more complex at high load levels around sites of internal discontinuity, such as the location of reinforcing bar chairs and strain gages. A card-type clear plastic crack comparator was used to measure crack width.

Splitting cracks (parallel to the reinforcing bars) generally propagated from flexural cracks and first appeared at the splice ends, continuing toward the centerline of the beam. Splitting cracks were most commonly found on the tension face of the beam, although side splitting cracks often formed at higher load levels. Figure 3.4 shows bottom (as cast) and side splitting cracks that formed on specimen 8-8-XC1-2.5. Table 3.3 summarizes the loads, bar stresses, and flexural crack widths at the initiation of splitting cracks, excluding specimens in which no splitting cracks were observed before the final load step.

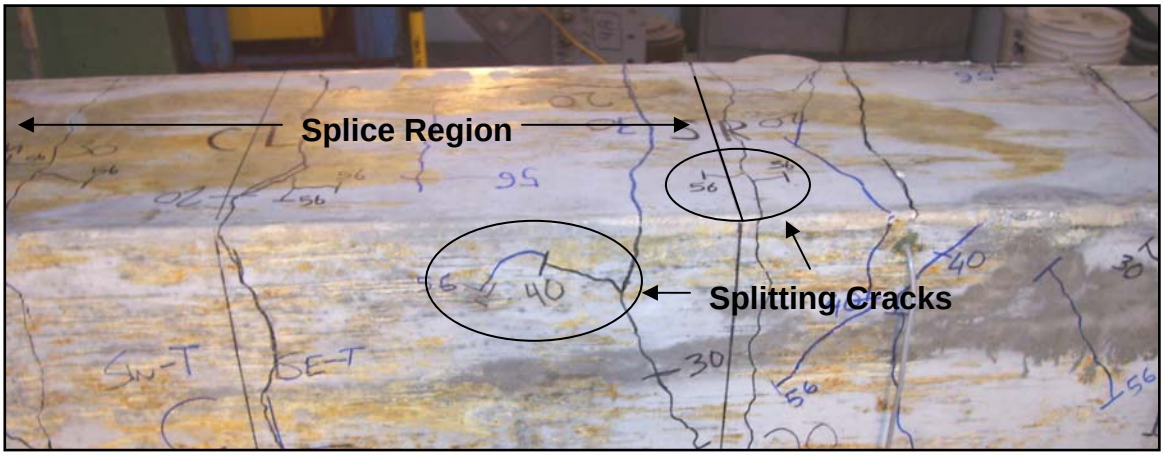

Figure 3.4 - Splitting cracks in specimen 8-8-XC1-2.5 at 56 kips total load

Table 3.3 - Load and bar stress at splitting crack initiation

Beam ID	f'_c	Nominal Section, b x h	Minimum Design Cover	Splice Length	Stirrups Confining Splice	At Splitting Crack Initiation		
						Total Load	Splice Stress	Flexural Crack Width
	(psi)	(in. x in.)	(in.)	(in.)	(ea.)	(kips)	(ksi)	(in.)
5-5-OC0-3/4	5,490	14 x 20	0.75	32	0	---	---	---
5-5-XC0-3/4	4,670			43	0	52	59	0.016
5-5-OC0-2d_b	5,490	35 x 10	1.25	18	0	---	---	---
5-5-XC0-2d_b	4,670			25	0	---	---	---
8-5-OC0-1.5	5,260	14 x 30	1.5	47	0	48	40	0.013
8-5-0C1-1.5	4,720				4	48	40	0.010
8-5-OC2-1.5	6,050				8	80	65	0.020
8-5-XC0-1.5	5,940			63	0	48	40	0.013
8-5-XC1-1.5	4,720				4	72	59	0.030
8-5-XC2-1.5	5,010				8	80	65	0.020
8-8-OC0-2.5	8,660	14 x 21	2.5	27	0	---	---	---
8-8-OC1-2.5	7,790				2	30	39	0.013
8-8-OC2-2.5	7,990				5	44	55	0.020
8-8-XC0-2.5	7,990			36	0	32	41	0.016
8-8-XC1-2.5	7,790				2	40	51	0.020
8-8-XC2-2.5	8,660				5	68	85	0.030
11-8-OC0-2	9,370	24 x 26	2	58	0	64	38	0.016
11-8-OC1-2	9,370				4	64	38	0.020
11-8-OC2-2	8,680				8	64	38	0.016
11-8-XC0-2	9,910			79	0	64	38	0.016
11-8-XC1-2	9,910				4	64	40	0.013
11-8-XC2-2	8,680				8	80	48	0.020

In beams with confining transverse reinforcement, splitting cracks typically initiated at higher loads than for beams without confining transverse reinforcement. Generally, splitting cracks initiated in unconfined beams at a bar stress of about 40 ksi, while splitting cracks initiated in confined beams at bar stresses between 55 and 85 ksi. In four beams with unconfined splices, splitting cracks were not observed before the last load step at which it was safe to approach the beam. Three of these four were the slab specimens with No. 5 tension reinforcement.

During tests of the Series 5 specimens (beams with No. 11 bars), splitting cracks were also noted near the supports at higher bar stresses. After testing of Series 5 specimens with high confinement, splitting cracks were observed along the majority of the beam length, even away from the regions of highest moment. Splitting cracks

were noted within one foot of the loading apparatus (at the end of the beam) on specimen 11-8-XC2-2.

3.5 Comparisons with Development Length Equations

Comparisons between the test results and the corresponding predictions for the 64 specimens that failed in bond at all three universities are presented in this section. The specimens are divided into two groups – those without confining transverse reinforcement and those with. Reported are the average, standard deviation, range, and coefficient of variation of the test/prediction ratios for both ACI 318-05 [Eq. (1.2)] and ACI 408R-03 [Eq. (1.1)]. For specimens with confining transverse reinforcement, the transverse reinforcement terms for Eq. (1.2) and Eq. (1.1) are limited to 2.5 and 4, as required by the respective equations.

3.5.1 Unconfined Specimens

The results for 31 unconfined specimens are presented in this section, 10 from KU, 13 from UT and 8 from NCSU. Of these, 10 are slab specimens with four splices each and 21 are standard beam-splice specimens.

University of Kansas Specimens

The ten unconfined specimens from KU had an average test/prediction ratio of 0.83 when compared with ACI 318-05 and 0.95 when compared with ACI 408R-03, indicating that both equations overestimate splice strength and are unconservative. In addition to more severely overestimating splice strength, ACI 318-05 also exhibits more scatter, with a coefficient of variation of 0.19, compared to 0.10 for ACI 408R-03, as can be seen in Table 3.4.

Table 3.4 - Comparison of tested and predicted bar stresses at failure for unconfined KU specimens

Specimen	Test	ACI 318-05		ACI 408R-03	
	Stress (ksi)	Stress (ksi)	Test/ Prediction	Stress (ksi)	Test/ Prediction
5-5-OC0-3/4	77	105	0.73	80	0.96
5-5-XC0-3/4	82	122	0.68	91	0.91
5-5-OC0-2d_b	87	78	1.12	77	1.12
5-5-XC0-2d_b	91	94	0.97	90	1.01
8-5-OC0-1.5	78	84	0.93	77	1.01
8-5-XC0-1.5	90	120	0.75	99	0.90
8-8-OC0-2.5	79	84	0.95	78	1.02
8-8-XC0-2.5	91	107	0.85	96	0.95
11-8-OC0-2	68	95	0.72	79	0.86
11-8-XC0-2	79	130	0.61	99	0.80
			0.83	Average	0.95
			0.16	Std. Dev.	0.09
			0.19	Coef. Var.	0.10
			1.12	Maximum	1.12
			0.61	Minimum	0.80

All Unconfined Specimens

Unconfined specimens for all universities showed similar results to those at KU. The average test/prediction ratios for ACI 318-05 and ACI 408R-03 are 0.87 and 0.98, respectively, indicating that while both equations overestimate the splice strength, ACI408R-03 is significantly more accurate. ACI 408R-03 also exhibits less scatter, as can be seen in Figure 3.5. The coefficients of variation for ACI 318-05 and ACI 408R-03 are, respectively, 0.20 and 0.11.

Since ACI 318-05 significantly overestimates splice strength and exhibits considerable scatter, it should not be used for the design of unconfined splices. Currently, 25 of the 31 specimens, or 81% have a test/prediction ratio lower than 1.0. A modification factor that reduces the number of tests with test/prediction ratios less than 1.0 to an acceptable number should be used if the equation is to be used in design. ACI 408R-03 has a test/prediction ratio much closer to unity, as well as less

scatter, but will also require a modification factor to be used safely for the design of unconfined splices.

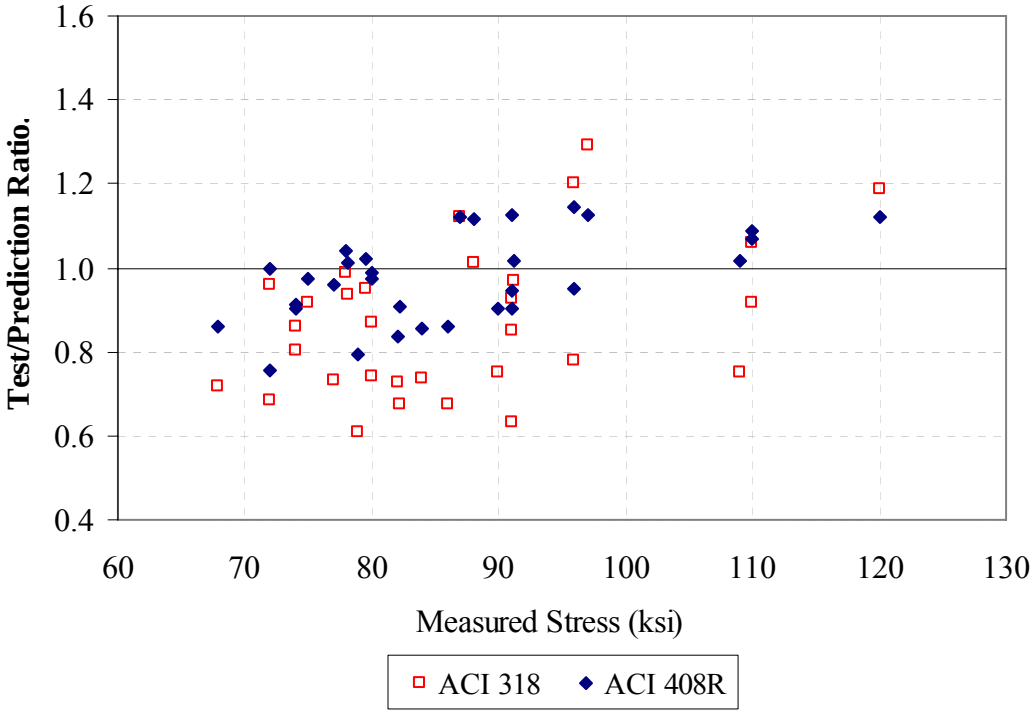

Figure 3.5 - Test/prediction ratios for unconfined specimens, all schools

Table 3.5 - Measured stresses and test/prediction ratios for unconfined specimens, all schools

Specimen	Test	ACI 318-05		ACI 408R-03	
	Stress (ksi)	Stress (ksi)	Test/ Prediction	Stress (ksi)	Test/ Prediction
University of Kansas					
5-5-OC0-3/4	77	105	0.73	80	0.96
5-5-XC0-3/4	82	122	0.68	91	0.91
5-5-OC0-2d_b	87	78	1.12	77	1.12
5-5-XC0-2d_b	91	94	0.97	90	1.01
8-5-OC0-1.5	78	84	0.93	77	1.01
8-5-XC0-1.5	90	120	0.75	99	0.90
8-8-OC0-2.5	79	84	0.95	78	1.02
8-8-XC0-2.5	91	107	0.85	96	0.95
11-8-OC0-2	68	95	0.72	79	0.86
11-8-XC0-2	79	130	0.61	99	0.80
University of Texas					
8-8-OC0-1.5	80	92	0.87	82	0.98
8-8-XC0-1.5	86	127	0.68	100	0.86
8-5-OC0-1.5	74	86	0.86	81	0.91
8-5-XC0-1.5	82	113	0.73	98	0.84
11-5-OC0-3	75	82	0.91	77	0.97
11-5-XC0-3	84	114	0.74	98	0.86
5-5-OC0-3/4	80	108	0.74	81	0.99
5-5-XC0-3/4	91	144	0.63	101	0.90
5-5-OC0-2d_b	88	87	1.01	79	1.11
5-5-XC0-2d_b	110	120	0.92	101	1.09
5-5-OC0-3d_b	97	75	1.29	86	1.13
5-5-XC0-3d_b	120	101	1.19	107	1.12
8-5-SC0-1.5	72	75	0.96	72	1.00
North Carolina State University					
8-5-OC0-2.5	96	80	1.20	84	1.14
8-5-XC0-2.5	110	104	1.06	103	1.07
8-8-OC0-1.5	91	98	0.93	81	1.12
8-8-XC0-1.5	109	145	0.75	107	1.02
11-5-OC0-2	74	92	0.80	82	0.90
11-5-XC0-2	72	105	0.69	95	0.76
11-8-OC0-3	78	79	0.99	75	1.04
11-8-XC0-3	96	123	0.78	101	0.95
			0.87	Average	0.98
			0.18	Std. Dev.	0.11
			0.20	Coef. Var.	0.11
			1.29	Maximum	1.14
			0.61	Minimum	0.76

3.5.2 Confined specimens

Thirty-three specimens with two levels of confinement are presented here. The confinement levels increase the unconfined splice strength, by 20 ksi for confinement level 1, and by 40 ksi for confinement level 2, as discussed in Section 2.2.3.

University of Kansas Specimens

The University of Kansas tested 12 specimens with splices confined by transverse reinforcement. The comparisons in Table 3.5 show that, on average, ACI 318-05 and ACI 408R-03 provide average test/prediction ratios of 1.01 and 1.02, respectively. Although the test/prediction ratios are both extremely close to 1.00, ACI 318-05 exhibits significantly more scatter, with a coefficient of variation of 0.19, compared with 0.10 for ACI 408R-03.

Table 3.6 - Comparison of tested and predicted bar stresses at failure for confined KU specimens

Specimen	Test	ACI 318-05		ACI 408R-03	
	Stress (ksi)	Stress (ksi)	Test/ Prediction	Stress (ksi)	Test/ Prediction
8-5-OC1-1.5	124	108	1.15	99	1.24
8-5-XC1-1.5	129	142	0.90	118	1.09
8-5-OC2-1.5	127	122	1.04	127	1.00
8-5-XC2-1.5	143	149	0.96	136	1.06
8-8-OC1-2.5	89	79	1.12	89	0.99
8-8-XC1-2.5	111	106	1.05	111	1.00
8-8-OC2-2.5	115	80	1.43	101	1.14
8-8-XC2-2.5	117	112	1.05	129	0.91
11-8-OC1-2	95	106	0.90	95	1.01
11-8-XC1-2	107	161	0.66	126	0.85
11-8-OC2-2	124	128	0.97	122	1.01
11-8-XC2-2	137	164	0.84	141	0.98
			1.01	Average	1.02
			0.19	Std. Dev.	0.10
			0.19	Coef. Var.	0.10
			1.43	Maximum	1.24
			0.66	Minimum	0.85

All Confined Specimens

Thirty-three specimens at KU, UT, and NCSU had splices confined by transverse reinforcement. The comparisons for confined splices are shown in Figure 3.6 and Table 3.7. In this case, the average test/prediction ratios for ACI 318-05 and ACI 408R-03 are, respectively, 1.10 and 1.06. As observed for unconfined splices, the comparisons for confined splices in Table 3.7 show that the design equation in ACI 318-05 results in a higher standard deviation and range of test/prediction ratios than does the equation in ACI 408R. The respective coefficients of variation are 0.21 and 0.10 for ACI 318-05 and ACI 408R-03.

Average test/prediction ratios just greater than 1.0 indicate that both equations slightly underestimate the splice strength. Comparisons for ACI 318-05 using the database in ACI 408R-03 have a higher test/prediction ratio, 1.26, for the more than 250 specimens confined by transverse reinforcement, and a coefficient of variation of 0.24.

The expression from ACI 408R-03 is intended for analysis purposes, such that a test/prediction ratio close to 1.0 represents a good match with the test results. The test/prediction ratio and coefficient of variation of the MMFX Grade 100 reinforcing steel were 1.06 and 0.10, respectively. Comparisons for the confined specimens in the ACI 408R-03 database produce an average test/prediction ratio of 1.00 and a coefficient of variation 0.12. Comparisons by Zuo and Darwin (1998), using an equation close to Eq. (1.1), showed that the test/prediction ratio averaged 1.00 for all confined specimens but averaged 1.10 for specimens in which the longitudinal steel yielded prior to bond failure. Zuo and Darwin (1998) speculated that the higher bond strength for the bars that yielded was due to increased slip along the splice length resulting in the mobilization of more transverse reinforcement. This may also be the case for MMFX steel with its highly nonlinear stress-strain curve.

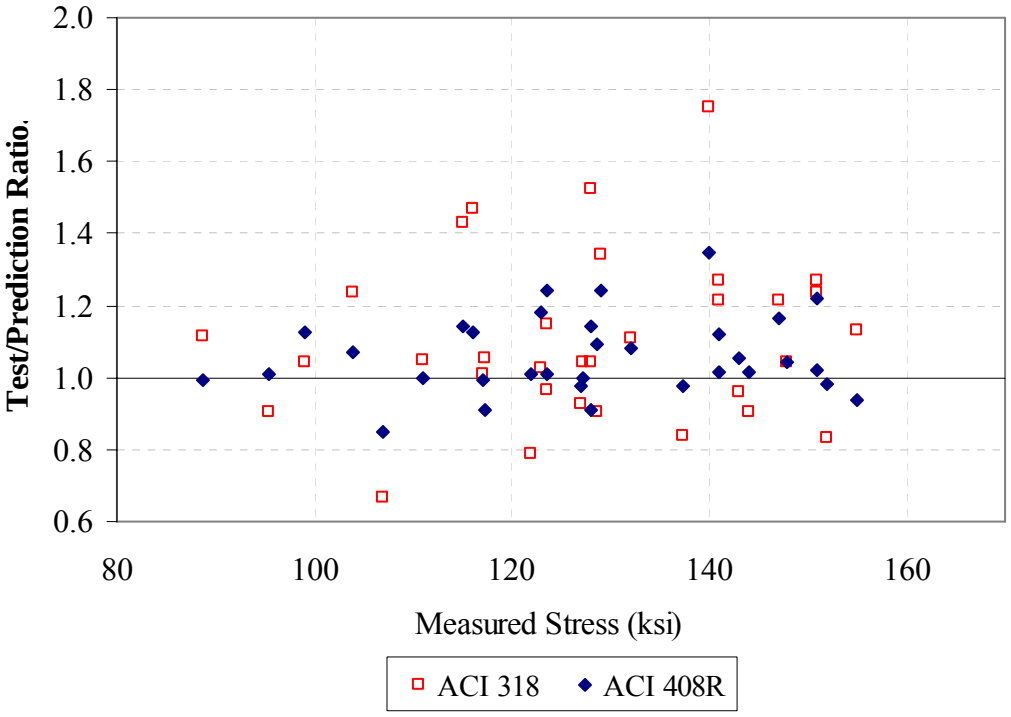

Figure 3.6 - Test/Prediction ratios for confined specimens, all schools

Table 3.7 - Measured stresses and test/prediction ratios for confined specimens, all schools

Specimen	Test	ACI 318-05		ACI 408R-03	
	Stress (ksi)	Stress (ksi)	Test/ Prediction	Stress (ksi)	Test/ Prediction
University of Kansas					
8-5-OC1-1.5	124	108	1.15	99	1.24
8-5-XC1-1.5	129	142	0.90	118	1.09
8-5-OC2-1.5	127	122	1.04	127	1.00
8-5-XC2-1.5	143	149	0.96	136	1.06
8-8-OC1-2.5	89	79	1.12	89	0.99
8-8-XC1-2.5	111	106	1.05	111	1.00
8-8-OC2-2.5	115	80	1.43	101	1.14
8-8-XC2-2.5	117	112	1.05	129	0.91
11-8-OC1-2	95	106	0.90	95	1.01
11-8-XC1-2	107	161	0.66	126	0.85
11-8-OC2-2	124	128	0.97	122	1.01
11-8-XC2-2	137	164	0.84	141	0.98
University of Texas					
8-8-OC1-1.5	123	120	1.03	104	1.18
8-8-XC1-1.5	122	155	0.79	121	1.01
8-8-OC2-1.5	147	121	1.21	126	1.17
8-8-XC2-1.5	144	159	0.91	142	1.01
8-5-OC2-1.5	141	111	1.27	126	1.12
8-5-XC2-1.5	148	142	1.04	142	1.04
11-5-OC1-3	104	84	1.24	97	1.07
11-5-XC1-3	117	116	1.01	118	0.99
11-5-OC2-3	128	84	1.52	112	1.14
11-5-XC2-3	141	116	1.22	139	1.01
8-5-SC1-1.5	99	95	1.04	88	1.13
8-5-SC2-1.5	129	96	1.34	104	1.24
North Carolina State University					
8-5-OC1-2.5	140	80	1.75	104	1.35
8-8-OC1-1.5	151	122	1.24	124	1.22
8-8-XC1-1.5	152	182	0.84	155	0.98
11-5-OC1-2	132	119	1.11	122.0	1.08
11-5-OC2-2	151	119	1.27	148.0	1.02
11-5-XC1-2	127	137	0.93	130.0	0.98
11-5-XC2-2	155	137	1.13	165.0	0.94
11-8-OC1-3	116	79	1.47	103.0	1.13
11-8-XC1-3	128	123	1.04	141.0	0.91
			1.10	Average	1.06
			0.23	Std. Dev.	0.11
			0.21	Coef. Var.	0.10
			1.75	Maximum	1.35
			0.66	Minimum	0.85

3.6 Comparisons with Development Length Equations based on Confinement Term

The equations for bond strength for bars confined by transverse reinforcement limit the confining reinforcement terms in the equations to distinguish the point where increased confinement results in a change from a splitting to a pullout failure. For ACI 318-05 [Eq. (1.2)] the term $\left(\frac{c_b + K_{tr}}{d_b}\right)$ is limited to 2.5. For ACI 408R-03 [Eq. (1.1)], the term $\left(\frac{c\omega + K_{tr}}{d_b}\right)$ is limited to 4.0. At this point, the effect of additional confinement provided by either increased concrete cover or increased confining transverse reinforcement is assumed to result in no increase in bond strength. In design, confinement terms greater than 2.5 [Eq. (1.2)] or 4.0 [Eq. (1.1)] are reduced to 2.5 and 4.0, respectively. For analysis purposes, specimens with confinement terms greater than 2.5 [Eq. (1.2)] or 4.0 [Eq. (1.1)] are typically disregarded.

Table 3.8 - Effect of changing the confinement limit for ACI 318-05

Upper limit on $\left(\frac{c_b + K_{tr}}{d_b}\right)$	ACI 318-05						
	Number of Tests	Maximum	Minimum	Average	Standard Deviation	Coefficient of Variation	Percent with T/P <1.0
2.50	33	1.75	0.66	1.10	0.23	0.21	30%
2.75	33	1.59	0.66	1.02	0.19	0.19	48%
3.00	33	1.46	0.66	0.97	0.16	0.17	58%
None	33	1.09	0.66	0.89	0.11	0.12	79%
$\left(\frac{c_b + K_{tr}}{d_b}\right)$ > 2.5 disregarded	7	1.04	0.66	0.88	0.13	0.15	71%

Twenty-six of thirty-three specimens had confinement terms in ACI 318-05 [Eq. (1.2)] greater than 2.5, with a maximum of 5.0. As shown in Table 3.8, increasing the upper limit of the confinement term reduces the test/prediction ratio and the coefficient of variation. Changing the confinement limit from 2.5 to 2.75 reduces the test/prediction ratio from 1.10 to 1.02, and the coefficient of variation

from 0.21 to 0.19. Eliminating the confinement limit changes the average test/prediction ratio from 1.10 to 0.89, and reduces the coefficient of variation from 0.21 to 0.12. Increasing the confinement limit also has the effect of increasing the number of specimens with test/prediction ratios less than 1.0.

Discarding specimens with confinement terms in ACI 318-05 greater then 2.5 reduced the number of test specimens in the sample from 33 to 7 and reduced the test/prediction ratio from 1.10 to 0.88. The coefficient of variation decreased as well, changing from 0.21 to 0.15.

Table 3.9 - Effect of changing the confinement limit for ACI 408R-03

Upper limit on $\left(\frac{c\omega + K_{tr}}{d_b}\right)$	ACI 408R-03						
	Number of Tests	Maximum	Minimum	Average	Standard Deviation	Coefficient of Variation	Percent with T/P <1.0
4.0	33	1.35	0.85	1.058	0.108	0.102	27%
4.5	33	1.24	0.85	1.044	0.102	0.098	30%
5.0	33	1.24	0.85	1.039	0.100	0.096	30%
none	33	1.24	0.85	1.038	0.099	0.095	30%
$\left(\frac{c\omega + K_{tr}}{d_b}\right)$ > 4.0 disregarded	26	1.24	0.85	1.051	0.096	0.091	27%

Seven specimens had confinement terms in Eq. (1.1) (ACI 408R-03) greater than 4.0. Of these, only one was greater than 5.0. As shown in Table 3.9, increasing the upper limit on the confinement term has the effect of reducing both the test/prediction ratio and coefficient of variation, as it did for Eq. (1.2). For confinement limits of 4.5 and 5.0, the test/prediction ratios dropped from 1.058 (for a limit of 4.0) to 1.044 and 1.039, respectively. The coefficients of variation also decreased, from 0.102 (for 4.0) to 0.098 and 0.096 for limits of 4.5 and 5.0.

Discarding specimens with confinement terms in ACI 408R-03 greater then 4.0 reduced the number of test specimens in the sample from 33 to 26 and brought the test/prediction ratios closer to 1.0, reducing the test/prediction ratio from 1.06 to 1.05. The coefficient of variation decreased as well, changing from 0.10 to 0.09.

Increasing the limit on the confinement term in each equation reduces the test/prediction ratio by more adequately accounting for the effects of the confining transverse reinforcement. The confining reinforcement term has more effect on Eq. (1.2) than Eq. (1.1). Increasing the confinement limit to 5.0 for Eq. (1.1) reduces the average test/prediction ratio by 1.8%, and increasing the confinement limit for Eq. (1.2) by 0.5 reduces the average test/prediction ratio by 12%.

It should be noted that the current comparisons apply only to the tests in this study, while the limits applied in Eq. (1.1) and (1.2) were developed for bars that were developed or spliced at lower stresses.

CHAPTER 4

SUMMARY AND CONCLUSIONS

4.1 Summary

The bond strength of MMFX Grade 100 reinforcing steel is evaluated with respect to equations in ACI 408R-03 and ACI 318-05 for the estimation of bond strength and bond design, respectively, for conventional reinforcing steel. MMFX Grade 100 reinforcing steel has a nominal yield strength of 100 ksi, whereas the reinforcing steel used to calibrate the equations in ACI 408R-03 and ACI 318-05 had nominal yield strengths ranging from 40 to 75 ksi.

The study consisted of 69 full scale beam-splice specimens tested in four-point bending, placing the splice within a constant moment region. Of these, 64 failed in bond and are included in this report. Ten specimens were cast as slabs with four splices without confining transverse reinforcement, 21 were conventional beam-splice specimens with two splices without confining transverse reinforcement, and the remaining 33 had two splices with confining transverse reinforcement. The University of Kansas tested 22 specimens, the University of Texas, 25 (all of which failed in bond) and North Carolina State University, 22 (of which 17 failed in bond).

Factors affecting bond that were included in this study were splice length, amount of confinement, bar spacing, bar size, concrete cover, and concrete compressive strength. Splice length ranged from 15 in. to 91 in. for specimens without confining transverse reinforcement, and from 27 in. to 91 in. for specimens with confining transverse reinforcement. Bar spacing was typically at least twice the concrete clear cover. Bar sizes studied were No. 5, No. 8, and No. 11. Beams were tested at two concrete compressive strengths, 5000 and 8000 psi. Specimens with splices not confined by transverse reinforcement had maximum bar stresses at failure ranging from 68 to 120 ksi. Specimens with splices confined by transverse reinforcement had maximum bar stresses at failure ranging from 89 to 155 ksi.

Test specimens were divided into unconfined and confined specimens, without and with confining transverse reinforcement, respectively, for the purposes of analysis. For the unconfined specimens, the average test/prediction ratios when compared to ACI 408R-03 and ACI 318-05 were 0.98 and 0.87, with coefficients of variation of 0.20 and 0.11, respectively. For the confined specimens, the respective average test/prediction ratios were 1.06 and 1.10, with coefficients of variation of 0.10 and 0.21.

4.2 Observations and Conclusions

The following observations and conclusions are based on the test results presented in this report.

1. Lap splices using MMFX Grade 100 reinforcing steel developed stresses between 68 and 155 ksi.
2. The use of confining transverse reinforcement increases splice strength and deformation capacity.
3. The development length equation found in ACI 318-05 is not suitable for use in design of unconfined or confined splices without the addition of a modification factor.
4. The development length equation found in ACI 408R-03 is suitable for analysis for both unconfined and confined splices using MMFX Grade 100 reinforcing steel.
5. The development length equation in ACI 408R-03 exhibited significantly less scatter than that in ACI 318-05.
6. Increasing the limit on the confinement term for both ACI 318-05 and ACI 408R-03 increased the accuracy and decreased the scatter for both equations.

4.3 Recommendations for Future Study

1. Further testing should be conducted using strain gages to study the effects of bars slip on spliced Grade 100 reinforcing steel. Strain gage data was only available for 6 of the 22 tests conducted at KU.
2. The effects of changing the confinement limit should be studied with beam-splice specimens utilizing Grades 60 and 75 steel to determine if the same observation that increasing the confinement limit decreases the test/prediction ratio holds true for all steel.

REFERENCES

ACI Committee 318, 2005. “Building Code Requirements for Structural Concrete (ACI 318-05) and Commentary (ACI 318R-05)”, American Concrete Institute, Farmington Hills, MI.

ACI Committee 408, 2003. “Bond and Development of Straight Reinforcing Bars in Tension (ACI 408-03) and Commentary (ACI 408R-03)”, American Concrete Institute, Farmington Hills, MI.

Ansley, M., 2002, “Investigation into the Structural Performance of MMFX Reinforcing,” *Research Report,* Florida Department of Transportation, Structures Research Center. 7 pp.

ASTM A 615/A 615M, 2007, “Standard Specification for Deformed and Plain Carbon-Steel Bars for Concrete Reinforcement,” ASTM International, West Conshohocken, PA.

ASTM A 1035/A 1035M, 2006, “Standard Specification for Deformed and Plain, Low-carbon, Chromium, Steel Bars for Concrete Reinforcement,” ASTM International, West Conshohocken, PA.

ASTM C 39/C 39M, 2005, “Standard Test Method for Compressive Strength of Cylindrical Concrete Specimens,” ASTM International, West Conshohocken, PA.

ASTM C 172, 2004, “Standard Practice for Sampling Freshly Mixed Concrete.” ASTM International, West Conshohocken, PA.

ASTM C 617, 1998, "Standard Practice for Capping Cylindrical Concrete Specimens," ASTM International, West Conshohocken, PA.

Darwin, D. and Graham, E. 1993, "Effect of Deformation Height and Spacing on Bonds Strength of Reinforcing Bars," *ACI Structural Journal*, V. 90, No. 6, Nov.-Dec., pp. 646-657.

Darwin, D.; Tholen, M. L; Idun, E. K.; and Zuo, J., 1996a, "Splice Strength of High Relative Rib Area Reinforcing Bars," *ACI Structural Journal*, V. 93, No. 1, Jan.-Feb., pp. 95-107.

Darwin, D., Zuo, J., Tholen, M., and Idun, E., 1996b, "Development Length Criteria for Conventional and High Relative Rib Area Reinforcing Bars," *ACI Structural Journal,* V. 93, No. 3, May-June, pp 347- 359.

Dawood, M.; Seliem, H.; Hassan, T.; and Rizkalla, S., 2004, "Design Guidelines for Concrete Beams Reinforced with MMFX Microcomposite Reinforcing Bars," *Proceedings of the International Conference on Future Vision and Challenges for Urban Development*, Cairo, Egypt, Dec. 20-22, 12 pp.

Donnelly, K., 2007, "Behavior of Minimum Length Splices of High-Strength Reinforcement," *Thesis*, University of Texas, Dept. of Civil, Architectural, and Environmental Engineering, Austin, TX. 27 pp.

El-Hacha, R and Rizkalla, S. H., 2002, "Fundamental Material Properties of MMFX Steel Bars," *Research Report*, RD-02/04, North Carolina State University, Constructed Facilities Laboratory, Raleigh, NC, July, 62 pp.

Orangun, C. O.; Jirsa, J. O.; and Breen, J. E., 1977, "Reevaluation of Test Data on Development Length and Splices," ACI Journal, *Proceedings* V. 74, No. 3, Mar., pp. 114-122.

Peterfreund, S., 2003, "Development Length of Micro-composite (MMFX) Steel Reinforcing Bars used in Bridge Deck Applications," *Senior Honors Project*, University of Massachusetts Amherst. 52 pp.

Rizkalla, S., El-Hacha, R., and Elagroudy, H., 2006, "Bond Characteristics of High-Strength Steel Reinforcement," *ACI Structural Journal*. V. 103, No. 6, Nov. - Dec., pp 771-782.

Zuo, J., and Darwin, D., 2000, "Splice Strength of Conventional and High Relative Rib Area Bars in Normal and High-Strength Concrete," *ACI Structural Journal*, V. 97, No. 4, July-Aug., pp 630-641.

APPENDIX A
MATERIAL PROPERTIES

Table 6.1 - Nominal Concrete Mix Designs

Material	Designation	Mix		Unit
		5 ksi	8 ksi	
Cement	Ashgrove Type I/II; ASTM C 150	564	756	lb
Fine Aggregate, SSD	Kansas River Sand; ASTM C 33/KDOT S-1	1377	1415	lb
Coarse Aggregate, SSD	3/4 in. Crushed Limestone; KDOT LS-3	1823	1635	lb
Water	KDOT Potable	247	242	lb
Water Reducer	W.R. Grace Adva100; ASTM C 494 Type F	0-18	0	oz.
	W.R. Grace AdvaFlex; ASTM C 494 Type F	0	75	oz.
W/C Ratio		0.46	0.32	--
Target Slump		3	5	in.
Compressive Strength		4,670 - 6,050	7,790 - 9,910	psi
Target Age		10	7	days
Actual Age		6-42	4-7	days

*Batch weights reported per CY

Table 6.2 - Aggregate Properties

Material	Bulk Specific Gravity		Fineness Modulus	Unit Weight	Absorption OD
	OD	SSD			
3/4 in. Crushed Limestone KDOT LS-3	2.48	2.57	--	99 pcf	3.3%
Kansas River Sand; KDOT S-1	2.60	2.62	2.65	--	0.6%

Table 6.3 - HRWRA Properties

Material	Specific Gravity	Percent Solids
W.R. Grace Adva 100 ASTM C 494 Type F	1.1	30-34%
W.R. Grace AdvaFlex ASTM C 494 Type F	1.0	28-32%

Table 6.4 - MMFX Grade 100 Reinforcement Deformation Properties

Bar Size (No.)	Average Rib Height (in.)	Average Rib Spacing (in.)	Relative Rib Area
5.00	0.0386	0.415	0.0767
8.00	0.0644	0.680	0.0838
11.00	0.0738	0.834	0.0797

APPENDIX B
TEST RESULT DETAILS

Table B.1 - Applied loads, moments, and calculated bar stress for beam-splice tests

Group	Specimen	Endspan to Support Distance	Load/Load Rod				Loading System Weight at Endspan		At Splice Ends						
									Moment from Self Weight		Moment from Applied Loads		Calculated Bar Stress		
			NE	SE	NW	SW	East	West	East	West	East	West	M-Φ	Strength	
		(ft.)	(kips)	(kips)	(kips)	(kips)	(kips)	(kips)	(k-ft)	(k-ft)	(k-ft)	(k-ft)	(ksi)	(ksi)	
1A	**5-5-OC0-3/4**	4	17.3	17.2	16.8	17.0	0.370	0.384	1.4	1.4	137.8	138.8	77.0	73.9	
1B	**5-5-XC0-3/4**	4	18.0	18.5	18.5	18.0	0.370	0.384	1.7	1.7	147.5	147.5	82.2	79.5	
2A	**5-5-OC0-2db**	4	8.8	8.9	8.4	8.5	0.370	0.384	1.6	1.6	70.4	71.1	86.9	83.1	
2B	**5-5-XC0-2db**	4	8.7	9.8	9.2	9.5	0.370	0.384	1.7	1.7	75.8	75.7	91.2	87.8	
3A	**8-5-OC0-1.5**	5.5	23.5	24.5	24.0	24.0	0.370	0.384	3.3	3.3	266.8	267.0	78.1	75.1	
	8-5-OC1-1.5	5.5	37.8	38.6	38.5	37.9	0.370	0.384	3.3	3.3	422.3	422.3	123.5	122.1	
	8-5-OC2-1.5	5.5	39.5	40.2	40.4	39.6	0.370	0.384	3.3	3.3	440.9	441.6	127.3	125.4	
3B	**8-5-XC0-1.5**	5.5	27.6	28.6	27.5	27.6	0.370	0.384	4.0	4.0	306.5	309.8	90.0	87.0	
	8-5-XC1-1.5	5.5	39.6	40.3	39.9	39.2	0.370	0.384	3.9	3.9	438.1	440.5	128.7	127.5	
	8-5-XC2-1.5	5.5	45.5	46.1	46.1	45.7	0.370	0.384	4.9	4.9	506.7	506.2	143.0	141.4	
4A	**8-8-OC0-2.5**	5.5	16.0	16.0	16.1	15.6	0.370	0.384	1.9	1.9	176.7	177.2	79.5	75.9	
	8-8-OC1-2.5	5.5	17.0	18.0	18.2	17.8	0.370	0.384	2.0	2.0	197.9	196.7	88.7	85.3	
	8-8-OC2-2.5	5.5	22.7	23.4	24.2	22.8	0.370	0.384	1.9	1.9	258.6	257.5	115.0	112.3	
4B	**8-8-XC0-2.5**	5.5	18.1	18.3	18.7	17.7	0.370	0.384	2.1	2.1	202.3	202.3	91.1	87.7	
	8-8-XC1-2.5	5.5	22.9	22.0	22.3	21.5	0.370	0.384	2.1	2.1	245.4	247.1	111.0	108.1	
	8-8-XC2-2.5	5.5	24.1	23.5	23.6	23.2	0.370	0.384	2.1	2.1	262.1	260.7	117.4	114.5	
5A	**11-8-OC0-2**	6.5	24.1	23.5	23.6	23.2	0.370	0.384	8.2	8.2	382.2	380.6	67.9	64.5	
	11-8-OC1-2	6.5	42.0	42.3	42.3	41.7	0.370	0.384	8.2	8.2	549.0	549.9	95.5	91.7	
	11-8-OC2-2	6.5	55.0	50.4	54.3	54.2	0.370	0.384	8.2	8.2	702.5	693.4	123.5	120.3	
5B	**11-8-XC0-2**	6.5	33.6	34.3	33.7	34.2	0.370	0.384	9.8	9.8	443.6	443.3	78.9	75.2	
	11-8-XC1-2	6.5	45.7	46.5	46.6	45.9	0.370	0.384	9.8	9.8	603.1	601.6	106.9	103.2	
	11-8-XC2-2	6.5	60.8	56.2	61.8	61.1	0.370	0.384	11.2	11.2	793.6	770.7	137.3	134.4	

B.1 Series 1

Both beams in Series 1 contained four No. 5 Grade 100 MMFX longitudinal tension bars. The beams contained a lap splice of length 32 in. (1A) or 43 in. (1B) centered at the midspan of the beam. The total span for Series 1 beams was 15 ft, with an internal span of 7 ft between supports. Series 1 beams were designed with four No. 5 Grade 60 bars as compression reinforcement. Both specimens contained 14 No. 4 closed stirrups spaced at 4 in. in the shear regions beyond the supports. Both specimens had unconfined splices.

The beams in this series were cast with a total depth of 21 in. in the shear regions on either end of the beam and a depth of 20 in. in the central region. The additional depth was added to provide adequate cover around the stirrups which, as designed, had ¼ in. or less clear cover to the tension face. The design cover of ¾ in. was maintained in the test region between supports by placing a 6-ft long, 1-in. thick insert centered at the middle of the beam. The bottom cover was 1 ¾ in. on the longitudinal steel and 1 ¼ in. on the stirrups in the end regions.

The ends of the insert were tapered at a 45º angle to minimize the effect of the stress concentration, although during testing flexural cracks did form at the notch before forming at other sites. The 6-ft length allowed the reduced section to be placed completely between the pin and roller support. In effect, the beams were cast as "dog-bone" sections, with the reduced section covering nearly the entire constant-moment region.

The major impacts of the increased section height in the end spans were a higher precracked section stiffness, the notch's localizing effect on the initial flexural crack location away from a point directly over the support, and better anchorage for the longitudinal and shear reinforcement in the end spans due to increased cover. Figure B.1, below, shows specimen 5-5-XC0-3/4, with its reduced section.

Cover was maintained within the splice region by suspending the spliced bars from a No. 4 cross bar, placed above the splices, which was then tied to standard 2-in. reinforcing bar chairs protruding up through the splices. Deformations were ground

down on the cross bar to reduce its bond to the surrounding concrete and limit any influence it may have had on splitting crack development. The cross bar was cut to prevent any overhang beyond the outermost bar in the exterior splices. Three chairs were used per cross bar, one between each splice.

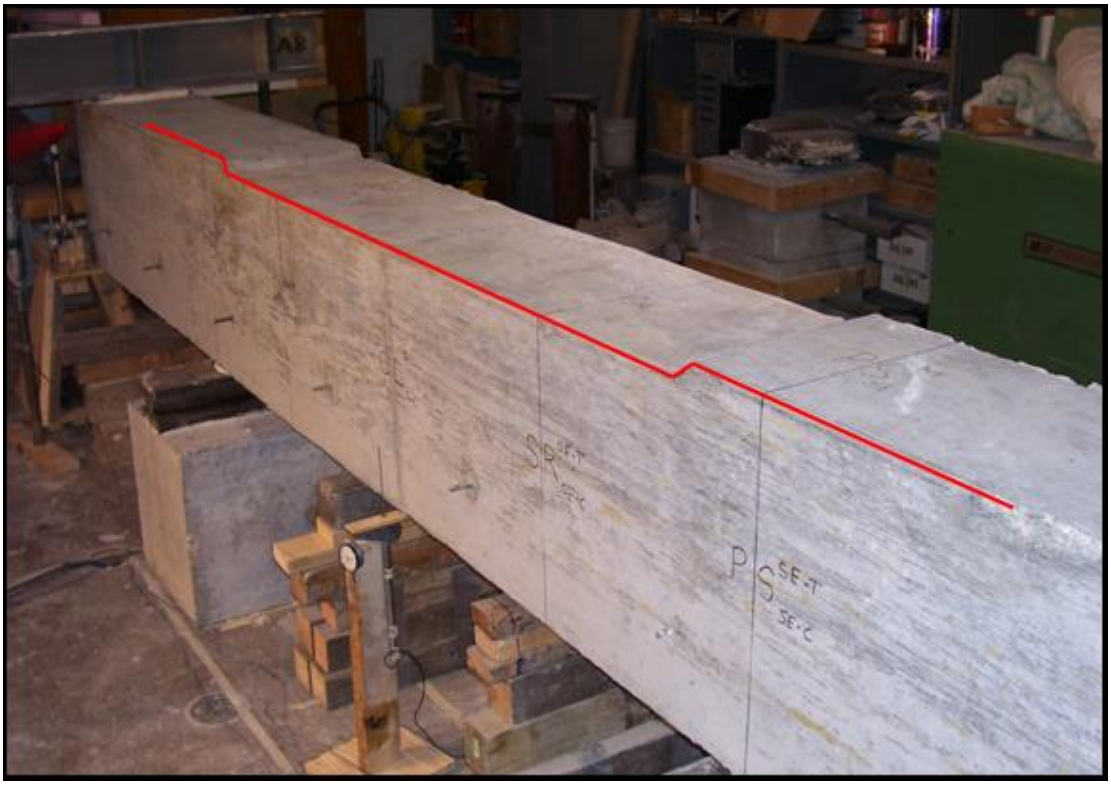

Figure B.1 - Specimen 5-5-XC0-3/4 with the reduced "dog-bone" section

The load-deflection behavior of the two beams in Series 1 is shown in Figure B.2, and is quite similar, despite the differences in splice length.

B.1.1 Group 1A

5-5-OC0-3/4

Specimen 5-5-OC0-3/4 failed due to the formation of splitting cracks in the splice region at a bar stress of 77.0 ksi, or 97% of the value predicted by ACI 408R. A photograph of the specimen following the completion of the test is shown in Figure B.3.

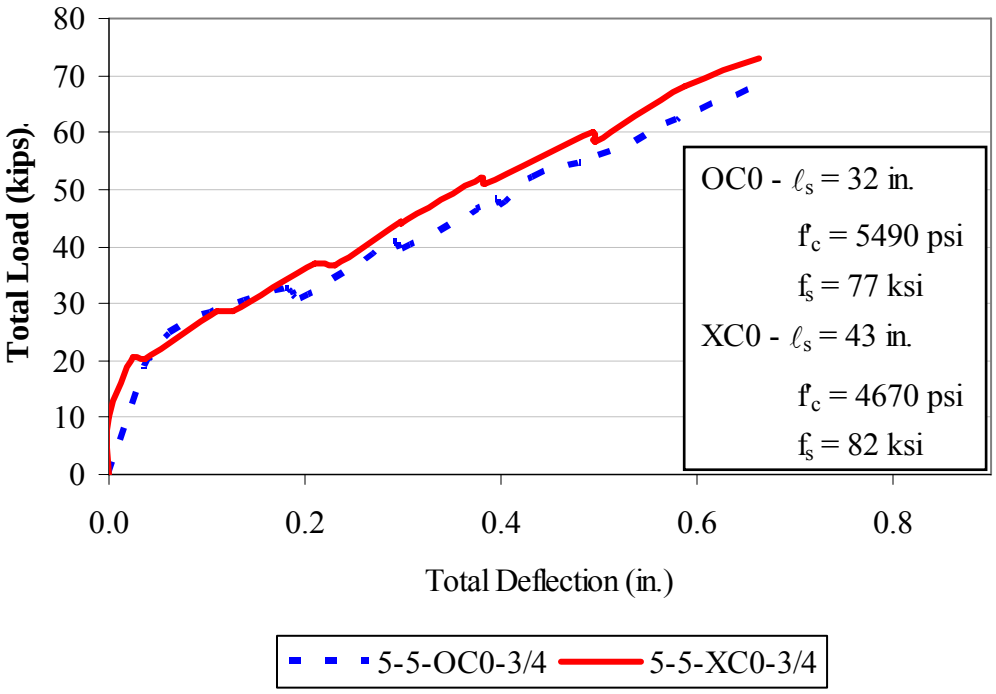

Figure B.2 - Load-deflection behavior of Series 1 beams

Figure B.3 - Beam 5-5-OC0-3/4 at the conclusion of the test

B.1.2 Group 1B

5-5-XC0-3/4

Specimen 5-5-XC0-3/4 failed due to the formation of splitting cracks in the splice region at a bar stress of 82.2 ksi, or 91% of the value predicted by ACI 408R. A photograph of the specimen following the completion of the test is shown in Figure B.4.

Figure B.4 - Beam 5-5-XC0-3/4 at the conclusion of the test

B.2 Series 2

Both beams in Series 2 contained four No. 5 Grade 100 MMFX longitudinal tension bars. Each bar was spliced with a lap length of 18 in. (2A) or 25 in. (2B) centered at the midspan of the beam. The total span for Series 2 beams was 15 ft, with an internal span of 7 ft between supports. Series 2 beams were designed without compression reinforcement, but contained four No. 4 Grade 60 bars to support the upper corners of the shear reinforcement. Both specimens contained fourteen rows of two No. 4 closed stirrups spaced at 4 in. in each shear region beyond the support, or 28 per end region. Both specimens had unconfined splices.

Series 2 beams were constructed using two separate reinforcement cages in each beam, with each consisting of two tension bars, and two compression bars with their own closed stirrups. This was done to provide shear reinforcement across the

entire width of the beam, rather than just at the exterior edges. The two cages were tied together using eight No. 4 bars per specimen.

Because of the 35 in. width of the specimens in Series 2, blockouts were used to reduce the width at the ends of the beam to accommodate the load rods, which were spaced 36 in. apart transversely. 9-in. long by 10-in. tall by 1½-in. deep blockouts were used, reducing the section width to 32 in. at both beam ends over the full height of the specimen. Specimen 5-5-XC0-2d_b used a further 45° transition for the blockout to make the end angled, giving it a total length of 10 ½ in., with 1 ½ in. of transition to the full width.

No chairs or other supports were placed within the splice region for either specimen in Series 2, given the very short splice length. Standard chairs were placed about 4 inches immediately outside of the splice region on both ends of each splice.

The load-deflection curves for the two beams in Series 2 are plotted in Figure B.5.

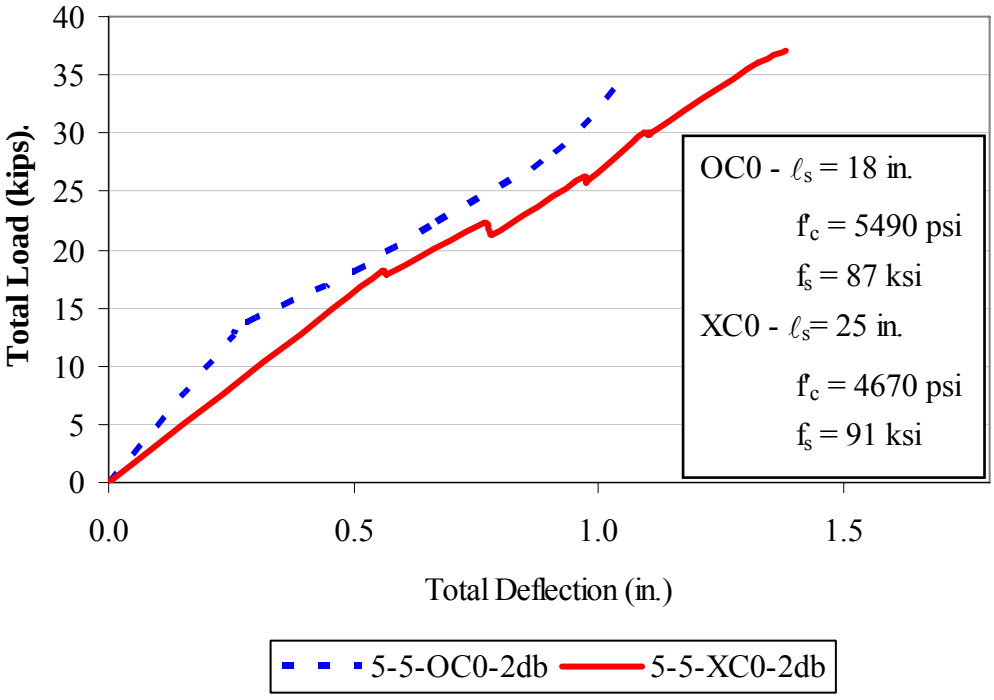

Figure B.5 - Load-deflection behavior of Series 2 beams

During testing on both specimens for Series 2, two distinct "pops" were audibly noted late into the loading, accompanied by small drops in load on the beam. It is believed that these were the exterior splices breaking, although no video or other suitable method exists to verify this. Given that the majority of the load was still being supported, however, loading was continued, and the reported breaking strengths are for the final peak loads on the beam, rather than potential individual splice strengths.

This phenomenon of exterior splices failing prior to failure of the entire specimen was also observed in the tests performed at UT on unconfined No. 5 bar beam-splice specimens, for which Series 1 and Series 2 beams are duplicates. Those conclusions are supported by strain gage data obtained by UT (Glass 2007).

B.2.1 Group 2A

5-5-OC0-2d_b

Specimen 5-5-OC0-2d_b failed due to the formation of bond splitting cracks in the splice region at a bar stress of 86.9 ksi, or 113% of the value predicted by ACI 408R. A photograph of the specimen following the completion of the test is shown in Figure B.6.

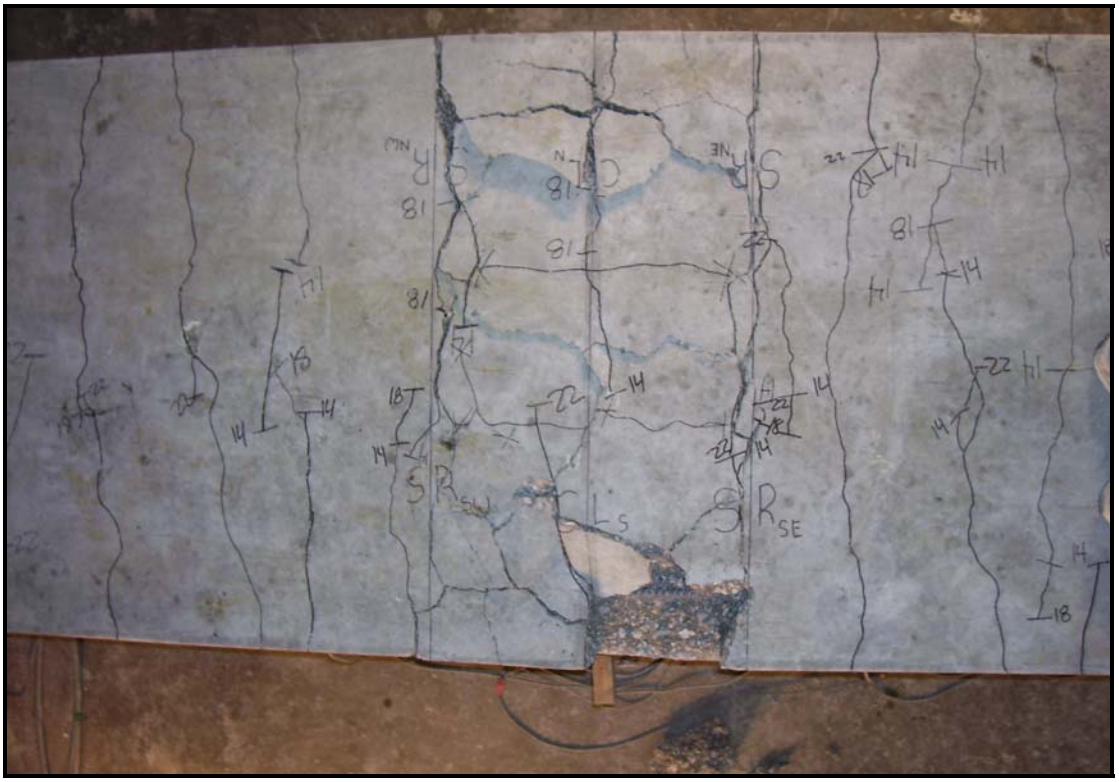

Figure B.6 - Beam 5-5-OC0-2d_b at the conclusion of the test, as viewed from above

B.2.2 Group 2B

5-5-XC0-2d_b

Specimen 5-5-XC0-2d_b failed due to the formation of bond splitting cracks in the splice region at a bar stress of 91.2 ksi, or 102% of the value predicted by ACI 408R. A photograph of the specimen following the completion of the test is shown in Figure B.7.

Figure B.7 - Beam 5-5-XC0-2d_b at the conclusion of the test

B.3 Series 3

The beams in Series 3 contained two No. 8 Grade 100 MMFX longitudinal tension bars. The beams contained lap splices with of lengths of 47 in. (4A) or 63 in. (4B) centered at the midspan of the beam. The total span for Series 3 beams was 21 ft, with an internal span of 10 ft between supports. Series 3 beams were designed without compression reinforcement, but contained two No. 4 Grade 60 bars to support the upper corners of the shear reinforcement. Specimen 8-5-XC2-1.5 was an exception because it was cast as a T-beam, as will be described below. All specimens contained 16 No. 4 closed stirrups spaced at 4.5 in. in each shear region beyond the support. The C0 specimens had unconfined splices, while the C1 and C2 specimens contained four and eight No. 4 closed stirrups within the splice region, respectively.

B.3.1 Group 3A

All beams in Group 3A had a splice length of 47 in. The load-deflection behavior is shown in Figure B.8.

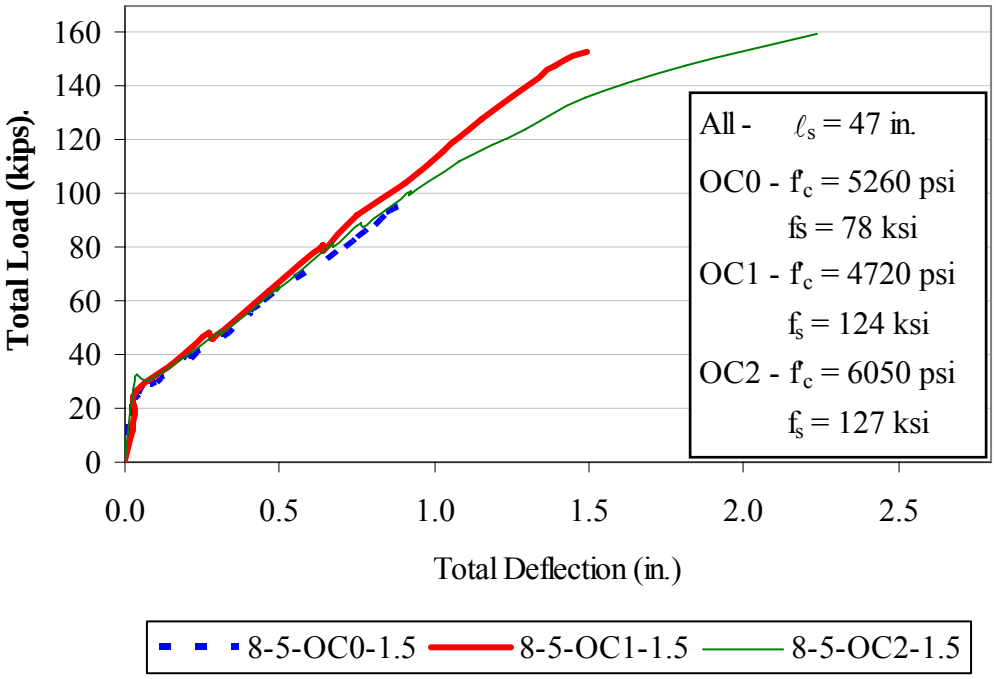

Figure B.8 - Load-deflection behavior of Group 3A beams

8-5-OC0-1.5

Specimen 8-5-OC0-1.5 failed due to the formation of bond splitting cracks in the splice region at a bar stress of 78.1 ksi, or 102% of the value predicted by ACI 408R. A photograph of the specimen following the completion of the test is shown in Figure B.9.

Figure B.9 - Beam 8-5-OC0-1.5 at the conclusion of the test

8-5-OC1-1.5

Specimen 8-5-0C1-1.5 failed due to the formation of bond splitting cracks in the splice region at a bar stress of 123.5 ksi, or 122 % of the value predicted by ACI 408R. A photograph of the specimen following the completion of the test is shown in Figure B.10.

Figure B.10 - Beam 8-5-OC1-1.5 at the conclusion of the test

8-5-OC2-1.5

Specimen 8-5-0C2-1.5 failed due to the formation of bond splitting cracks in the splice region at a bar stress of 127.3 ksi, or 99% of the value predicted by ACI 408R. A photograph of the specimen following the completion of the test is shown in Figure B.11.

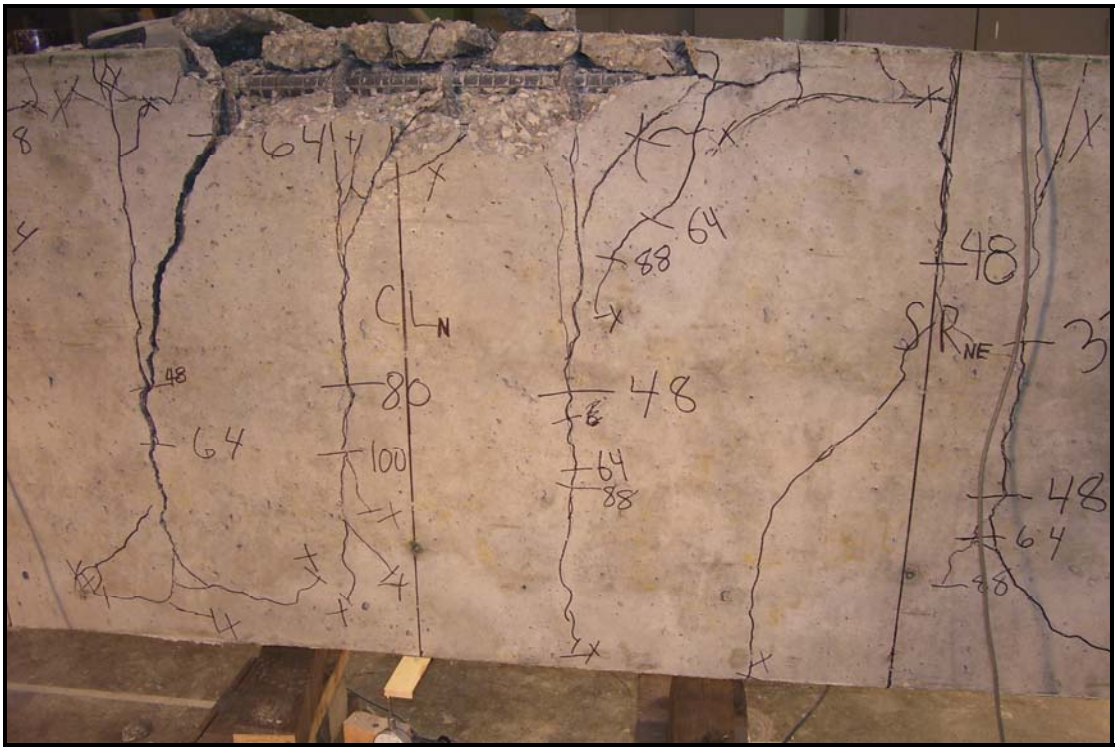

Figure B.11 - Beam 8-5-OC2-1.5 at the conclusion of the test

B.3.2 Group 3B

All beams in Group 3B had a splice length of 63 in. Specimen 8-5-XC2-1.5 was cast as a T-beam with a 28-in. wide, 7-in. deep flange. Specimen 8-5-XC2-1.5 also contained significantly more compression steel than the other beams in the group, 3.16 in.^{2} compared to the 0.40 in.^{2}. As expected, the load-deflection behavior was somewhat stiffer than that of the other two specimens in this group, as shown below in Figure B.12.

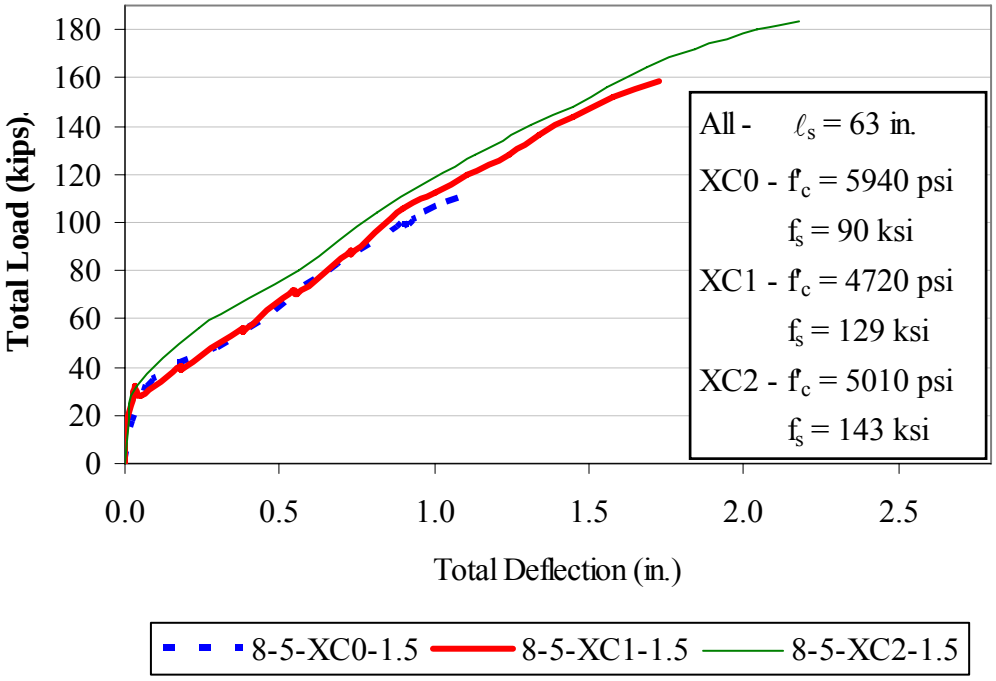

Figure B.12 - Load-deflection behavior of Group 3B beams

8-5-XC0-1.5

Specimen 8-5-XC0-1.5 failed due to the formation of bond splitting cracks in the splice region at a bar stress of 90.0 ksi, or 91% of the value predicted by ACI 408R. A photograph of the specimen following the completion of the test is shown in Figure B.13.

Figure B.13 - Beam 8-5-XC0-1.5 at the conclusion of the test

8-5-XC1-1.5

Specimen 8-5-XC1-1.5 failed due to the formation of bond splitting cracks in the splice region at a bar stress of 128.7 ksi, or 108% of the value predicted by ACI 408R. A photograph of the specimen following the completion of the test is shown in Figure B.14.

Figure B.14 - Beam 8-5-XC1-1.5 at the conclusion of the test

8-5-XC2-1.5

Specimen 8-5-XC2-1.5 failed by splitting in the splice region at a bar stress of 143.0 ksi, or 105% of the value predicted by ACI 408R. Only one splice appeared to have spalled the concrete, but upon failure of this splice, the beam lost approximately half the load it was carrying. It was later apparent that wooden blocks placed beneath the ends of the beam to prevent the ends from falling to the floor after failure were stacked high enough to prevent the second splice from failing. The test was discontinued at this point. A photograph of the specimen following the completion of the test is shown in Figure B.15.

Figure B.15 - Beam 8-5-XC1-1.5 at the conclusion of the test

In addition to being cast as a T-beam, specimen 8-5-XC2-1.5 differed from other beams in this program in that it contained U-stirrups with seismic hooks in the shear regions outside of the supports rather than the closed stirrups used in all other beams. U-stirrups were chosen to conserve material given that specimen 8-5-XC2-1.5 was a duplicate of a previously cast beam that failed in flexure. Closed stirrups were used, as normal, in the splice region for confinement.

The U-stirrups were closed with opposing U-stirrups that extended into the flanges to support two of the four No. 8 Grade 60 bars used as compression reinforcement. The other two No. 8 bars were placed within the hooks on the primary U-stirrups that confined the longitudinal steel in the ends. Two No. 3 bars were cast into specimen 8-5-XC2-1.5 at a depth of 5 ¼ in. from the top of the flange to anchor the hooks of the upper U-stirrups, but were not considered in the analysis of the beam for either tension or compression.

B.4 Series 4

All beams in Series 4 contained two No. 8 Grade 100 MMFX longitudinal tension bars. The beams had a lap splice of length 27 in. (4A) or 36 in. (4B) centered at the midspan of the beam. The total span for Series 5 beams was 21 ft with an internal span of 10 ft between supports. Series 4 beams contained two No. 8 Grade 60 bars as compression reinforcement. All specimens contained 15 closed stirrups spaced at 5 in. in each shear region beyond the support. C0 specimens had unconfined splices, while C1 and C2 specimens contained 2 and 5 No. 4 closed stirrups, respectively.

B.4.1 Group 4A

All beams in Group 4A had a splice length of 27 in. The load-deflection behavior is shown in Figure B.16

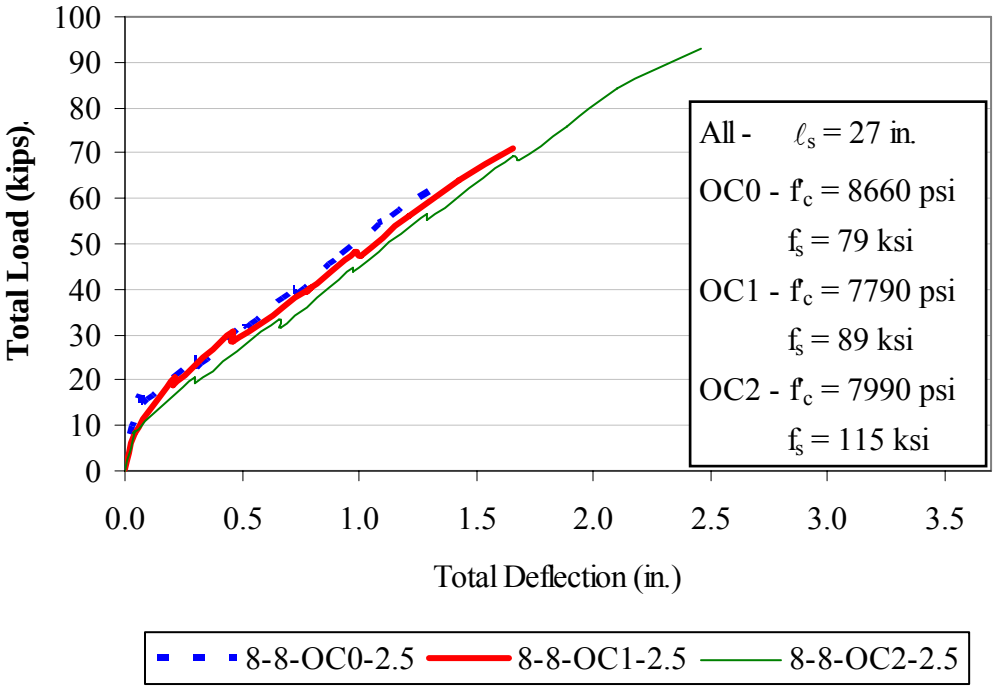

Figure B.16 - Load-deflection behavior of Group 4A beams

8-8-OC0-2.5

Specimen 8-8-OC0-2.5 failed due to the formation of bond splitting cracks in the splice region at a bar stress of 79.5 ksi, or 103% of the value predicted by ACI 408R. A photograph of the specimen following the completion of the test is shown in Figure B.17.

Figure B.17 - Beam 8-8-OC0-2.5 at the conclusion of the test

8-8-OC1-2.5

Specimen 8-8-OC1-2.5 failed due to the formation of bond splitting cracks in the splice region at a bar stress of 88.7 ksi, or 96% of the value predicted by ACI 408R. A photograph of the specimen following the completion of the test is shown in Figure B.18.

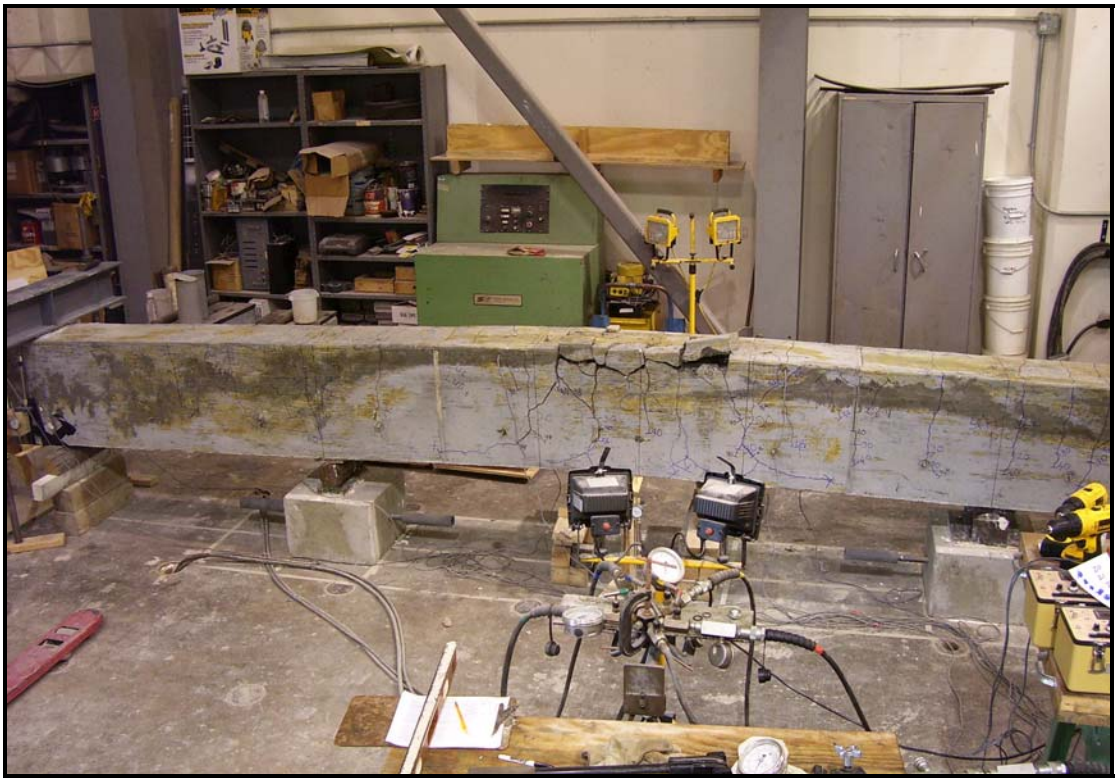

Figure B.18 - Beam 8-8-OC1-2.5 at the conclusion of the test

8-8-OC2-2.5

Specimen 8-8-OC2-2.5 failed due to the formation of bond splitting cracks in the splice region at a bar stress of 115.0 ksi, or 101% of the value predicted by ACI 408R. A photograph of the specimen following the completion of the test is shown in Figure B.19.

Figure B.19 - Beam 8-8-OC2-2.5 at the conclusion of the test

B.4.2 Group 4B

All beams in Group 4B had a splice length of 36 in. The load-deflection behavior is shown in Figure B.20.

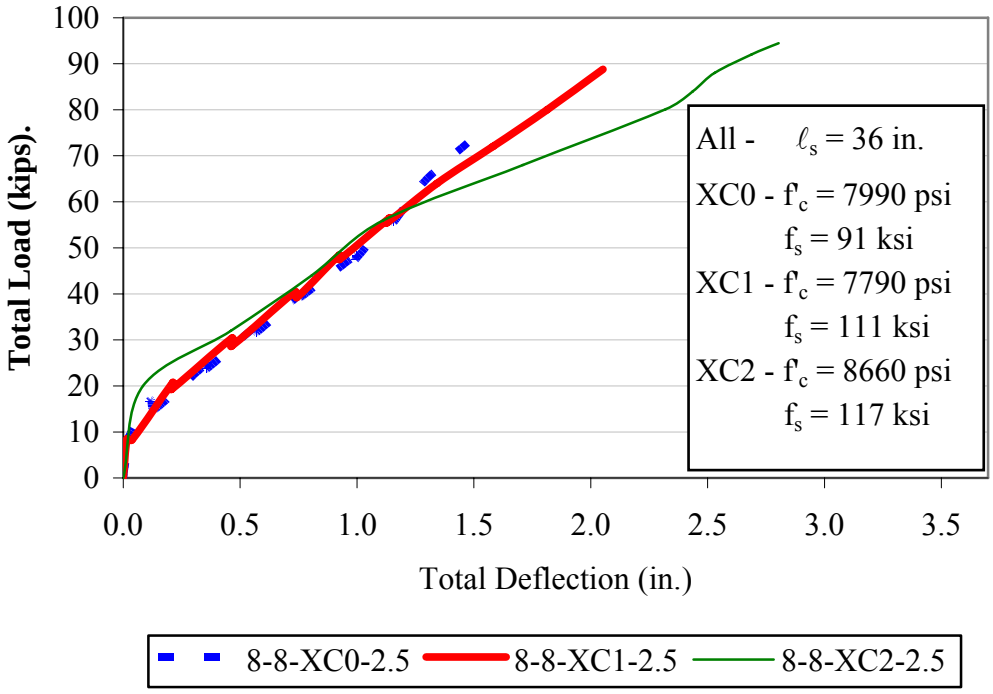

Figure B.20 - Load-deflection behavior of Group 4B beams

8-8-XC0-2.5

Specimen 8-8-XC0-2.5 failed due to the formation of bond splitting cracks in the splice region at a bar stress of 91.1 ksi, or 95% of the value predicted by ACI 408R. A photograph of the specimen following the completion of the test is shown in Figure B.21.

Figure B.21 - Beam 8-8-XC0-2.5 at the conclusion of the test

8-8-XC1-2.5

Specimen 8-8-XC1-2.5 failed due to the formation of bond splitting cracks in the splice region at a bar stress of 111.0 ksi, or 98% of the value predicted by ACI 408R. A photograph of the specimen following the completion of the test is shown in Figure B.22.

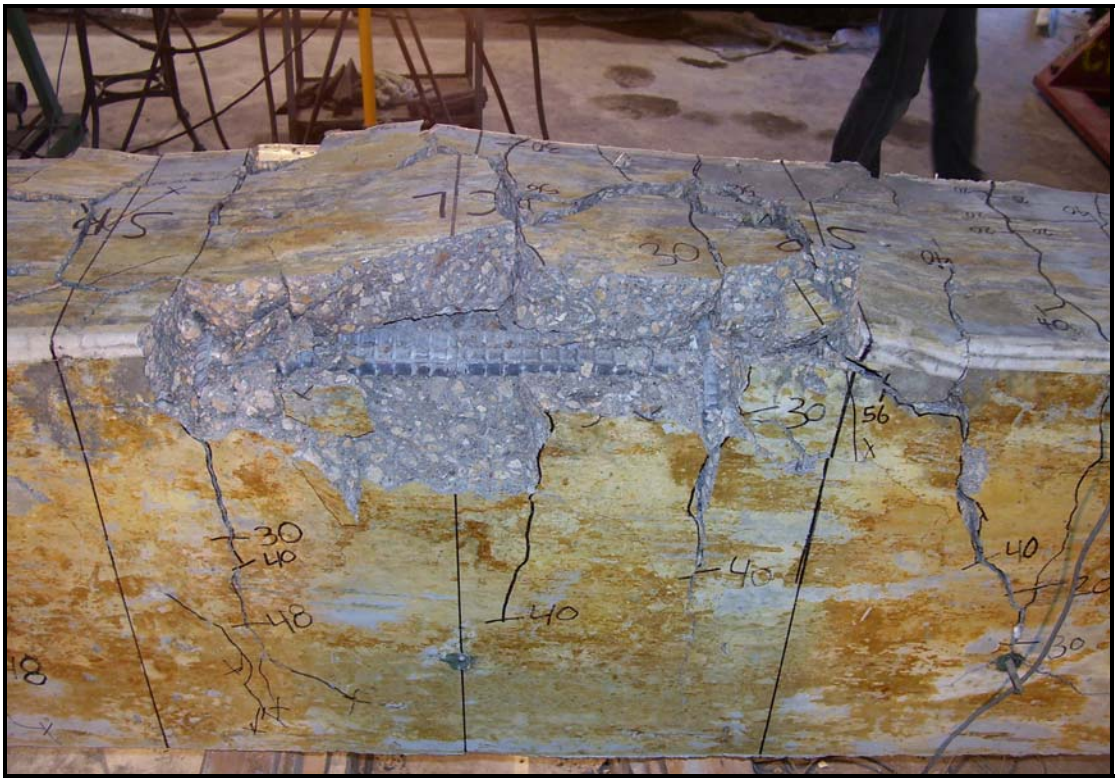

Figure B.22 - Beam 8-8-XC1-2.5 at the conclusion of the test

8-8-XC2-2.5

Specimen 8-8-XC2-2.5 failed due to the formation of bond splitting cracks in the splice region at a bar stress of 117.4 ksi, or 85% of the value predicted by ACI 408R. A photograph of the specimen following the completion of the test is shown in Figure B.23.

Figure B.23 - Beam 8-8-XC2-2.5 at the conclusion of the test

Specimen 8-8-XC2-2.5 was the sole specimen with a nominal target bar stress of 140 ksi that was not cast as a T-beam. Due to the first duplicate of specimen 8-5-XC2-1.5 experiencing a flexural failure at a bar stress near 140 ksi after the casting of this specimen, external stirrups were used in an attempt to confine the concrete at the highest moment regions away from the test region. Each external stirrup consisted of one C6x8.2 channel on both the top and bottom of the beam connected with ½-in. all-thread rod on each side of the beam. Four stirrups were used sequentially on each side of the splice region beginning at the edge of the bearing plate for the support and terminating roughly 10 in. from the end of the splice region. The bearing faces of the channels were attached with Hydrostone to the beam. A photograph showing these stirrups is shown in Figure B.24. The weight of the external stirrups was not included in the applied loads for moment calculation.

Figure B.24 - External stirrups used on beam 8-8-XC2-2.5

B.5 Series 5

All beams in Series 5 contained two No. 11 Grade 100 MMFX longitudinal tension bars. The beams had a lap splice of length 58 in. (5A) or 79 in. (5B) centered at the midspan of the beam. The total span for Series 5 beams was 24 ft with an internal span of 11 ft between supports. Series 5 beams were designed without compression reinforcement, but contained two No. 4 Grade 60 bars to support the upper corners of the shear reinforcement. Specimen 11-8-XC2-2, a T-beam, is an exception, as described below. All specimens contained 19 No. 5 closed stirrups spaced at 4.5 in. in each shear region beyond the support. The C0 specimens had unconfined splices, while the C1 and C2 specimens contained four and nine No. 4 closed stirrups, respectively.

B.5.1 Group 5A

All beams in Group 5A had a splice length of 58 in. The load-deflection behavior is shown below in Figure B.25

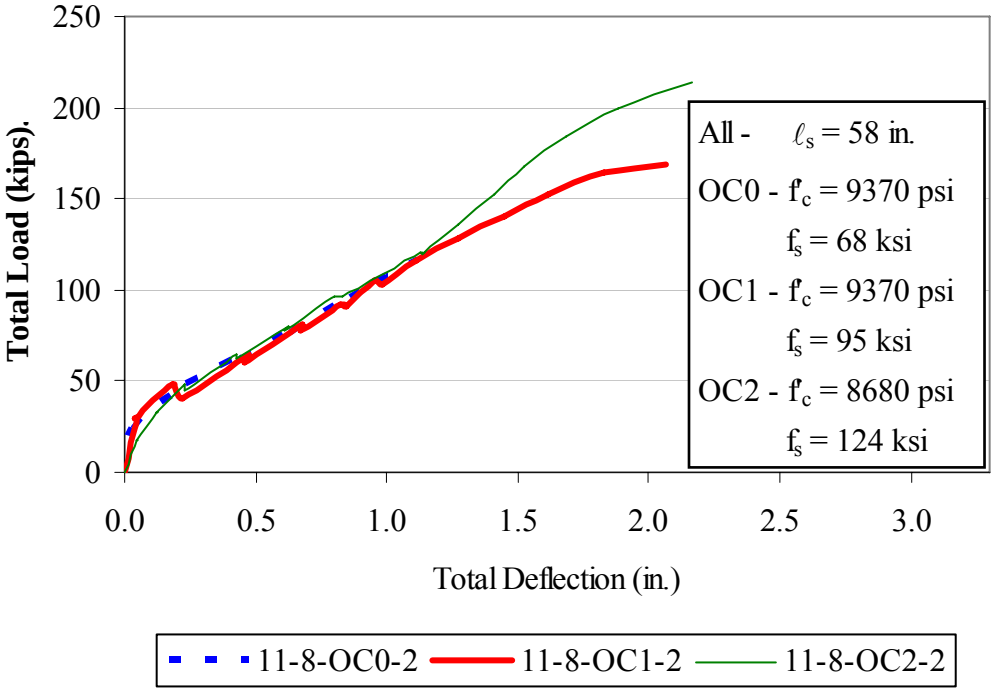

Figure B.25 - Load-deflection behavior of Group 5A beams

11-8-OC0-2

Specimen 11-8-OC0-2 failed due to the formation of bond splitting cracks in the splice region at a bar stress of 67.9 ksi, or 86% of the value predicted by ACI 408R. A photograph of the specimen following the completion of the test is shown in Figure B.26.

Figure B.26 - Beam 11-8-OC0-2 at the conclusion of the test

11-8-OC1-2

Specimen 11-8-OC1-2 failed due to the formation of bond splitting cracks in the splice region at a bar stress of 95.5 ksi, or 99% of the value predicted by ACI 408R. A photograph of the specimen following the completion of the test is shown in Figure B.27.

Figure B.27 - Beam 11-8-OC1-2 at the conclusion of the test, as viewed from above

11-8-OC2-2

Specimen 11-8-OC2-2 failed due to the formation of bond splitting cracks in the splice region at a bar stress of 123.5 ksi, or 100% of the value predicted by ACI 408R. A photograph of the specimen following the completion of the test is shown in Figure B.28.

Figure B.28 - Beam 11-8-OC2-2 at the conclusion of the test

Beam 11-8-OC2-2 was loaded to approximately 48 kips total load, at which point it was noted that the load distribution across the four load rods was uneven compared to that typically observed during tests. Additionally, at that load step, a severe and continual reduction in load was noted. As such, although the beam was well beyond the cracking load, all load was removed from the beam and the hydraulic system was completely reset and tightened. The beam was then reloaded from zero, and stable results were obtained for the remainder of the test.

B.5.2 Group 5B

All beams in Group 5B had a splice length of 79 in. Specimen 11-8-XC2-2 was cast as a T-beam with a 38-in. wide, 7-in. deep flange. Specimen 11-8-XC2-2 was also cast with significantly more compression steel, 3.56 in.^{2} compared with the 0.40 in.^{2} found in the other beams in the group. The load-deflection behavior is

somewhat stiffer for the T-beam compared to the other two specimens in the group, as shown in Figure B.29.

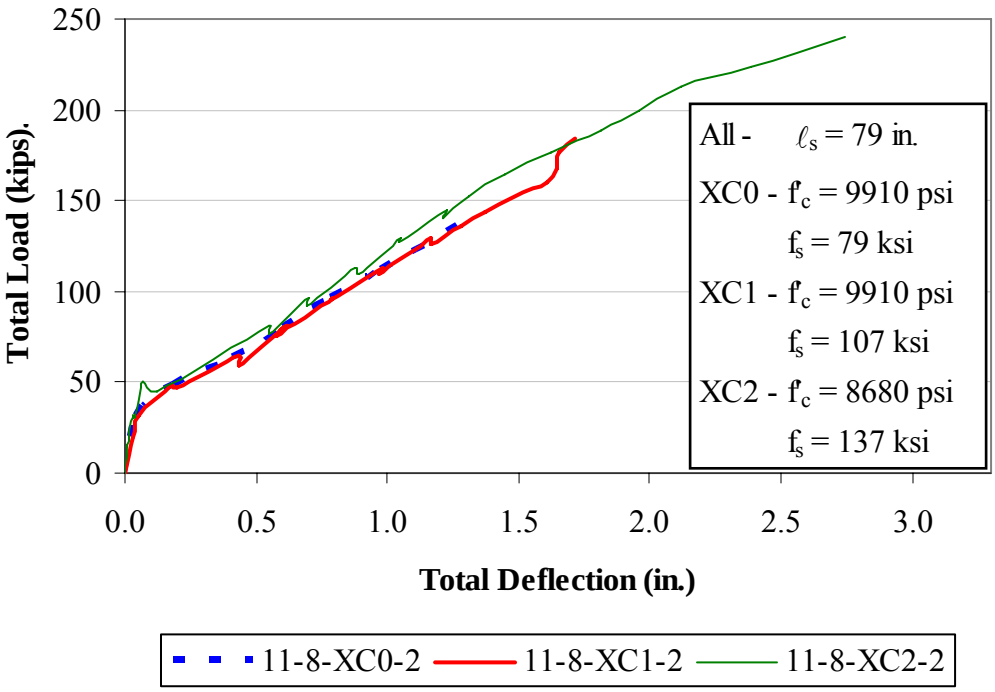

Figure B.29 - Load-deflection behavior of Group 5B beams

11-8-XC0-2

Specimen 11-8-XC0-2 failed due to the formation of bond splitting cracks in the splice region at a bar stress of 78.9 ksi, or 80% of the value predicted by ACI 408R. A photograph of the specimen following the completion of the test is shown in Figure B.30.

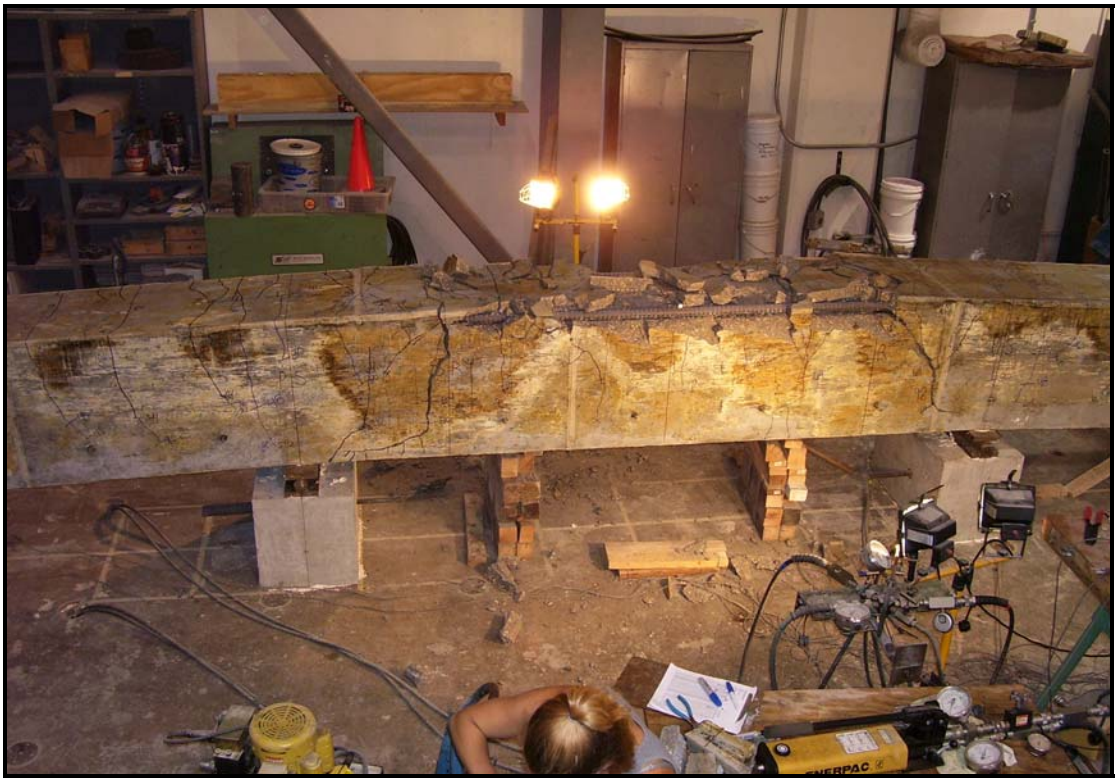

Figure B.30 - Beam 11-8-XC0-2 at the conclusion of the test

11-8-XC1-2

Specimen 11-8-XC1-2 failed due to the formation of bond splitting cracks in the splice region at a bar stress of 106.9 ksi, or 84% of the value predicted by ACI 408R. A photograph of the specimen following the completion of the test is shown in Figure B.31.

Figure B.31 - Beam 11-8-XC1-2 at the conclusion of the test

11-8-XC2-2

Specimen 11-8-XC2-2 failed due to the formation of bond splitting cracks in the splice region at a bar stress of 137.3 ksi, or 97% of the value predicted by ACI 408R. A photograph of the specimen following the completion of the test is shown in Figure B.32.

Figure B.32 - Beam 11-8-XC2-2 at the conclusion of the test

Given the 38-in. flange width of specimen 11-8-XC2-2, blockouts were used to reduce the flange width at the ends of the beam to accommodate the load rods, which were spaced 36 in. apart transversely. 9-in. long by 7-in. tall by 4-in. deep block-outs were used to eliminate a portion of the final nine inches of the flange, resulting in a final reduced flange width at both ends of approximately 30 in.